Materials Advances

ROYAL SOCIETY OF CHEMISTRY

REVIEW

View Article Online
View Journal | View Issue

Cite this: *Mater. Adv.*, 2023, 4, 3907

Nanoceramics-reinforced chitosan scaffolds in bone tissue engineering

Ganesh Harini,† Ramanathan Bharathi,† Aravind Sankaranarayanan, † Abinaya Shanmugavadivu and Nagarajan Selvamurugan *

In recent years, there has been a substantial rise in the use of nanomaterials in tissue engineering applications. Nanostructured scaffolds with cells provide a more structurally supportive environment like natural bone microarchitecture and govern cell proliferation, differentiation, and migration, resulting in the development of functional tissues. Chitosan is a promising and suitable biomaterial due to its remarkable qualities, such as biocompatibility, biodegradability, and osteogenic potential. However, due to its poor mechanical strength, chitosan cannot be employed for load-bearing applications; thus, the combinatorial approach of chitosan and other biomaterials can be employed to overcome this limitation. Various bioceramics, such as bioinert (titanium, alumina, and zirconia), bioactive (bioglass and hydroxyapatite), and bioresorbable (tricalcium phosphate) materials, are used in bone tissue engineering. Fabricating these materials at nanoscale dimensions increases their surface area, thereby enhancing their cell adhesion. The review article aims to present a comprehensive discussion on the bioinert, bioresorbable, and bioactive nanoceramics-reinforced chitosan scaffolds in bone tissue engineering. This review article also highlights the *in vitro* and *in vivo* studies of existing and novel nanoceramics-reinforced chitosan scaffolds used in critical-bone defects and their advantages and challenges in bone defect regeneration.

Received 15th July 2023,
Accepted 3rd August 2023

DOI: 10.1039/d3ma00422h

rsc.li/materials-advances

1. Introduction

Bone is a vital component of the body's support system, characterised by its stiffness, hardness, and capability for regeneration. Primary functions of the bone include structural support for soft tissues, locomotion, provision of a protective site for blood cell production, and maintenance of

Department of Biotechnology, School of Bioengineering, College of Engineering and Technology, SRM Institute of Science and Technology, Kattankulathur, 603203, Tamil Nadu, India. E-mail: selvamun@srmist.edu.in; Tel: +91-9940632335
† These authors equally contributed.

G. Harini

G Harini is an undergraduate student of SRM Institute of Science and Technology, Chennai, Tamil Nadu, India, pursuing her BTech Biotechnology with a specialization in Regenerative Medicine. Her undergraduate research, under the guidance of Dr N Selvamurugan, focuses on the effect of phytocompound-loaded nanoparticles on anti-cancer activity and the development of a novel scaffold for bone tissue engineering. Harini's main areas of interest are nano biomaterials and regenerative medicine.

R. Bharathi

R Bharathi is an undergraduate student of SRM Institute of Science and Technology, Chennai, Tamil Nadu, India, pursuing her BTech Biotechnology with a specialization in Regenerative Medicine. Her undergraduate research, under Dr N Selvamurugan's guidance, focuses on using phytocompound-loaded nanocarriers for breast cancer apoptosis and a novel scaffold for bone tissue engineering. Bharathi's research interest primarily lies in epigenetics and stem cell technology.

acid–base balance.[1] It also serves as a mineral reservoir, thereby regulating the calcium and phosphate levels in the circulating body fluids.[2] In contrast to many other types of tissues, the bone possesses a remarkable ability to heal post-injury. In response to mechanical and metabolic changes, bone undergoes consistent modelling and remodelling processes of resorption and regeneration,[3] with the coordinated actions of primary cells, namely osteoblasts, osteoclasts, and osteocytes. Osteoclasts are involved in targeted damaged bone removal, followed by subsequent action by osteoblasts in new bone formation at the defect site. Osteoblasts further differentiate into osteocytes, which are involved in bone remodelling through the production of proteolytic enzymes.[2] The osteoblast-osteoclast interaction is significant in maintaining the healthy state of the bone, as the disturbed state of balance leads to bone-related disorders.[4] Bone defects can be divided into two types, mainly based on their size: critical and non-critical defects. Non-critical bone defects, which are less than 2.5 cm, have better healing capacity and do not require planned reconstruction or secondary surgery.[5] However, critical or intrinsic-large bone defects caused by clinical conditions, including osteomyelitis, tumour resection, infected non-unions, and post-traumatic bone loss,[6] cannot spontaneously heal during the patient's lifetime and requires medical intervention that could aid in the healing of the defect site and encourage bone regeneration.[5]

Bone grafts predominantly remain the most employed surgical technique, with a high clinical success rate for over a century in curing critical bone defects. Approximately two million bone grafting surgeries are conducted annually across the globe. In the United States, nearly 500 000 bone graft procedures are performed annually,[7] making bone grafts the second most prevalent tissue transplantation after blood transfusion. The global market for bone grafts and substitutes is anticipated to increase from $3.78 billion in 2022 to $5.71 billion by 2029 with a compound annual growth rate of 6.1%.[8] Successful bone grafts should have osteoconductive properties and stimulate osteogenesis at the defect site.[9] Based on the source of graft tissue, grafts can be characterised into autografts, allografts, and xenografts. Autografts are obtained from the same individual from specific bones such as the iliac crest, fibula, ribs, mandible, chin, or skull.[10] Autogenous bone grafting techniques remain the benchmark and are considered the gold standard due to their clinical advantages, such as high efficacy,[9] no risk of graft rejection owing to high histocompatibility,[11] no associated immune-related response, and no risk of disease transmission.[12] It is also well known for its osteoconductive and osteoinductive nature.[13] However, autogenous bone grafts have several drawbacks, including potential donor site morbidity, limited supply, sensory loss, pain infection, prolonged wound drainage, and necessary reoperation. The complication rate has been reported as 8.6%.[9,14]

On the other hand, allografts are harvested from a genetically different individual belonging to the same species.[14] They are a preferred substitute to autografts as they possess more advantages regarding convenient usage, lack of donor site morbidity and size diversification. Nevertheless, sterilisation and storage before the transplantation procedure impact the biological and mechanical properties of the graft, leading to the

S. Aravind

S Aravind is an undergraduate student of SRM Institute of Science and Technology, Chennai, Tamil Nadu, India, pursuing his BTech Biotechnology. Aravind's undergraduate research, under Dr N Selvamurugan's guidance, focuses on using phytocompound-loaded nanoparticles for triple-negative breast cancer cell apoptosis and a novel biocomposite scaffold for bone healing. His research interests include translational research and the use of biomaterials.

Abinaya Shanmugavadivu

Abinaya Shanmugavadivu is currently a PhD student under the guidance of Dr N. Selvamurugan. Her research focuses on designing and fabricating 3D-printed scaffolds and nanoparticle-mediated drug delivery for bone tissue engineering applications. Her primary areas of research interest include nanobiomaterials, drug delivery, and regenerative medicine.

N. Selvamurugan

Nagarajan Selvamurugan is currently working as a Professor at the Department of Biotechnology, College of Engineering and Technology, SRM Institute of Science and Technology, Chennai, India. His main areas of specialization are bone Biology, stem cell biology, cancer biology, and biomaterials. He published more than 169 papers in peer-reviewed journals, and holds an h-index of 66. He focuses on application-based research and hosted several government-funded projects from India's CSIR, ICMR, DBT, and DST.

loss of osteoinduction and osteogenic capability.[15] In contrast, xenografts involve the transplantation of bone tissue across different species and are prone to immune rejection.[14] The shortcomings of auto and allogenous bone grafts have led to the development of bone tissue engineering (BTE).

BTE is a promising novel alternative to traditional bone grafts. It employs the synergistic combination of the triad cells, biomaterials, and specific growth factors/signals[16] and aims to induce functional bone regeneration at the site of interest. A scaffold is a three-dimensional (3D) structural matrix that allows and stimulates the attachment and proliferation of osteogenic cells on its surface, provides all the requisite environmental cues, mimics the extracellular matrix (ECM) like the bone microenvironment *in vivo*, and allows new bone formation at the site of bone defect thereby, eventually disintegrate post healing of the site. Many fabrication technologies are evolving to create porous scaffolds using various biomaterials that can aid in the regeneration of bone tissues and even function as a drug delivery system.[17] A typical biomaterial should have the following characteristics: high strength, a reasonable rate of degradation, porosity, microstructure, flexibility, and required shape and size.[18] Any scaffold designed to function as a bone substitute should:

i. allow attachment, proliferation, and differentiation of the cells.

ii. allow efficient nutrient exchange and cell migration.

iii. provide high surface area.

iv. have an interconnected microporous network to enable vascularisation.

Compared to traditional bone grafts, tissue-engineered scaffolds do not give rise to postoperative complications at the surgery site.[19] Scaffolds could be composed of natural polymers, synthetic polymers, ceramics, or a combination of them, depending on the application and fabrication method. Natural polymers commonly used in BTE applications include collagen, gelatin (Gel), silk fibroin, chitosan (CS), hyaluronic acid, and alginate.[20] PCL (polycaprolactone), PLA (polylactic acid), PLGA (poly(lactic-*co*-glycolic acid)), and PLLA (poly(L-lactide)) are some of the synthetic polymers used.[21] Recently, there has been an increase in the usage of calcium phosphate-based ceramics due to their similarity to the mineral phase of bone.[22] Ceramic materials include biphasic calcium phosphate, β-tricalcium phosphate (β-TCP), hydroxyapatite (HAp), silica, titanium, and bioactive glass. These materials are bioresorbable and have the potential to form strong bonds with hard and soft tissues, thereby stimulating osteogenesis.[23]

Nanoceramics are ceramic materials composed of nanodimensional grains/crystallites with at least one aspect of the element below 100 nm. Also, nanoceramics show enhanced properties compared to their bulk material, such as remarkable mechanical properties, including incredible strength, excellent toughness, and high fatigue resistance.[24] The cost-friendly and facile fabrication methods of nanoceramics are the significant advantages researchers exploit for BTE applications. However, nanoscale bioceramics pose a significant disadvantage of being brittle.[25] Therefore, they can be synergistically combined with metals and polymers to overcome this drawback, improving their physiochemical properties. One such polymer that can be utilised is CS, a naturally derived biomaterial with immense applications in BTE, drug delivery, and wound healing.[26] Its similarity in the chemical structure with glycosaminoglycans, the significant component of the ECM of bone, has made it a well-qualified biomaterial for BTE.[27]

In spite of several advantages and extensive research findings on the combinatorial approach of nanoceramics-reinforced CS biocomposite scaffolds, to the best of our knowledge, there are no recent reviews on nanoceramics-reinforced CS scaffolds for applications in BTE. Thus, this review begins with a detailed discussion of nanoceramics and CS, followed by the applications, recent advances, and *in vitro* and *in vivo* evaluation of the osteogenic potential of various types of nanoceramics reinforced in CS scaffolds. Finally, we review the signalling pathways applicable to CS scaffolds incorporated with nanoscale ceramics and highlight the challenges and prospects of these successfully emerging biocomposite scaffolds for BTE applications.

2. Nanobioceramics – types and properties

Bioceramics refer to biocompatible ceramic materials used for specific biological or physiological functions in the human body. From dental implants to even heart valves, bioceramics can restore normal function, provide support, and aid in reconstructing the diseased site of interest. Calcium phosphates and bioactive glasses were the first bioceramics explicitly developed for bone repair.[28] Inorganic HAp nanocrystals ($Ca_5(PO_4)_3(OH)$) make up about 70% of the inorganic bone matrix, but there are also significant amounts of bicarbonate, citrate, magnesium, potassium, and sodium ions.[29] The development of bioceramics was inspired by the notion that scaffolds with a composition like that of the bone microenvironment would result in improved biocompatibility and lower the likelihood of rejection by the body.

The term 'bioceramics' covers a large class of non-metallic materials whose chemical compositions, bond types, bioactivity and properties vary widely, and are widely classified into three main groups, namely bioinert, bioactive, and bioresorbable ceramics.[30]

i. Bioinert ceramics typically have excellent mechanical and chemical stability *in vivo*; when implanted in living bone, they integrate into the bone tissue through ''contact osteogenesis''. Due to their excellent biocompatibility, there are no physiological responses or immunological rejections by bone tissue.[31]

ii. Bioactive ceramics, on the other hand, can chemically bind with living bone tissue and possess osteoconductive properties. Once introduced into the body, it induces a chemical interaction between the scaffold material interface and the tissue.[32] Bioactive materials are usually employed in tissue engineering to heal orthopedic, craniofacial, and dental osteomyelitis.[33]

iii. The third class of bioceramics, known for their bioresorbable property, are biodegradable ceramic materials that

undergo complete degradation upon contact with the surrounding tissue fluid.[34] One significant advantage of these ceramics is that they do not require secondary surgery to remove the implant from the site of the defect post-healing.

Bioceramics should not be allergenic, carcinogenic, or teratogenic. Some unique bioceramics properties that tissue engineers exploit to use as scaffolds are corrosion resistance, high compressive strength, hardness, and good biocompatibility.[25] Most importantly, due to their highly porous nature, there would be improved cell migration and interaction between the bioceramic scaffold and bone, post-implantation. The formation of apatite crystals on the surface of the biomaterials provides active sites for enhanced cell-biomaterial interaction. This, in turn, improves the efficiency of osseointegration and bone implant acceptance.[34]

Recently nanoscale biomaterials have been of great interest due to their unlimited potential to improve human health as BTE materials. Also, conventional micron-scale scaffolds designed for BTE applications neglect the properties of the bone tissue at the nanoscale level and fail to completely regenerate the bone defect site, resulting in some complications, including undesirable local tissue responses. Nanoscale structures have more surface area, leading to better cellular uptake and drug-loading efficiency than micron-scale structures.[35] The increased interest in research on nanoceramics is evidenced by the increasing number of documents published in the last few decades, spread across several subject areas including medicine and pharmacology (Fig. 1).

In a study conducted by Webster *et al.* to investigate the effect of HAp particle size in osteoblast function *in vitro*, it was reported that nanophase ceramics showed a higher percentage of osteoblast proliferation and adhesion compared to micron-sized ceramics.[36] Nanobioceramics can be synthesised in various forms, such as nanoparticles, nanowires, nanorods, and nanotubes,[37] depending on which the properties also widely differ. Several synthesis methods, such as microwave irradiation, nucleation, and crystallisation, have been reported to fabricate nanoceramics. Numerous studies have reported that

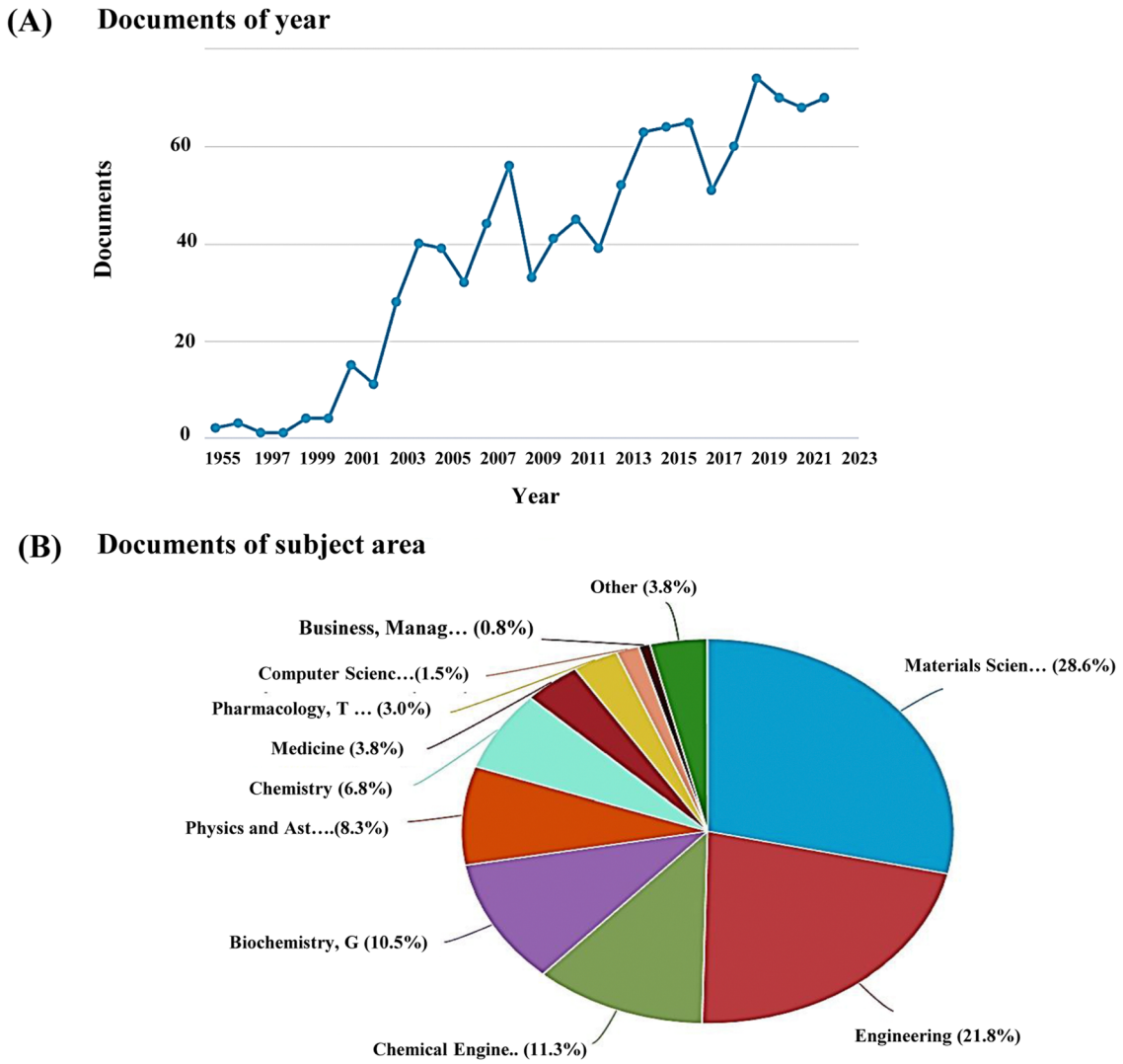

Fig. 1 (A) Publication trends and (B) subject areas analysed using Scopus database with keyword, 'nanoceramics' (last updated, 31 Dec 2022).

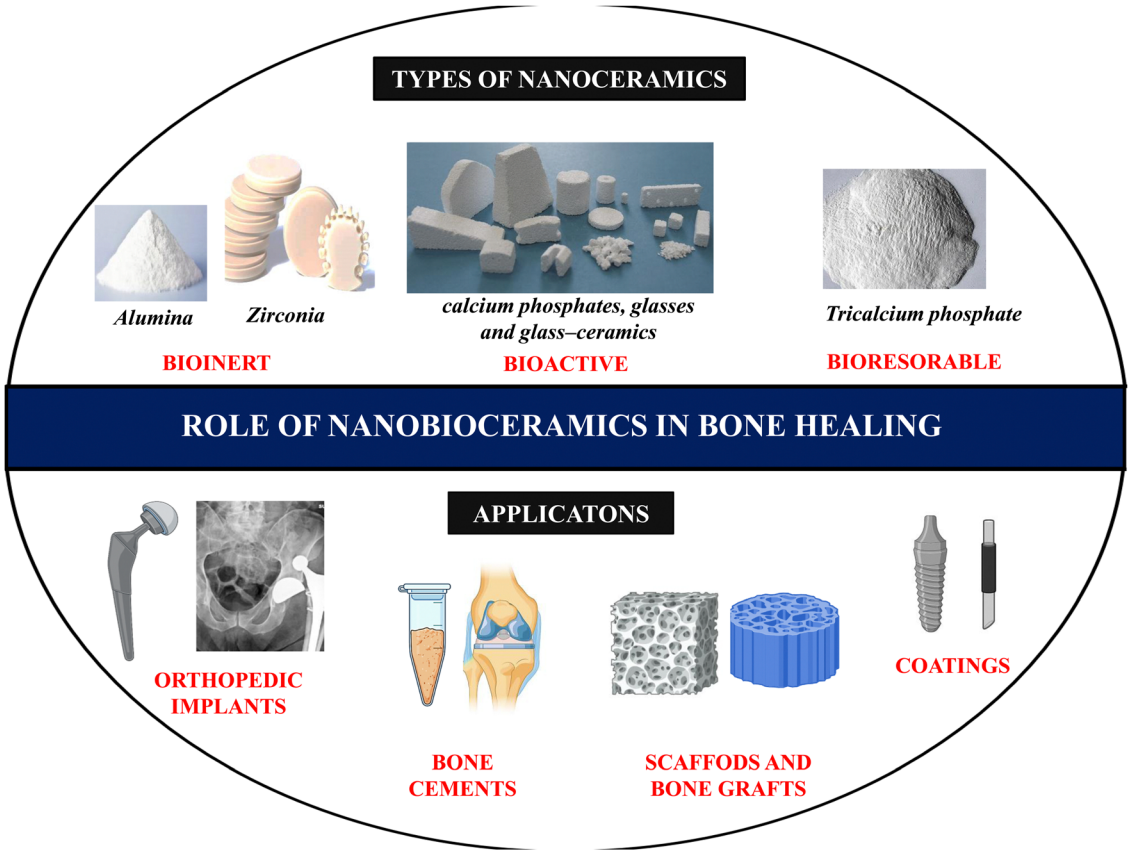

Fig. 2 Types of nanobioceramics and their application in bone healing.

incorporating nanoceramics into a polymeric scaffold of interest could be efficiently used in BTE applications.[38] Fig. 2 shows the role of nanoceramics in bone healing applications.

BTE greatly emphasizes the mechanical strength of the scaffolds, an extremely crucial parameter to be considered before the choice of biomaterial is made. Several impactful research works utilizing nanoceramics have stated significant improvement in the scaffolds' mechanical strength, toughness, and resistance upon their incorporation. Despite their brittle nature, ceramics, including alumina, ZrO_2, TiO_2, and bioglass, possess a high level of biocompatibility, and this attribute has been exploited for use in the creation of natural bone substitutes, implants, and hip arthroplasty. Calcium phosphate exhibits mechanical properties such as high brittleness, low impact resistance, and low tensile stress. However, its compressive strength is better than that of natural human bone, and it is widely reported to be suitable for non-load-bearing implants, defect filling, and coating applications.[39] Similarly, the application of 45S5 bioglass (BG) is restricted as a load-bearing scaffold material despite its outstanding ability to bond with bones and soft tissues due to its inherent brittleness.

Titanium and its alloys have exhibited superior biocompatibility and excellent corrosion resistance property. Fostad *et al.* reported TiO_2 scaffolds with high mechanical strength and high porosity using the polymer sponge method.[40] Therefore, by altering the manufacturing steps, designing composite blends, and governing morphological characteristics, the mechanical strength of the nanoceramics can be optimized for BTE applications.

3. Methods for synthesis of nanobioceramics

There are several methods for fabricating nanoceramics, such as the sol–gel technique, chemical vapour deposition, solvothermal and chemical precipitation methods (Fig. 3). These methods can produce various types of nanoceramics with diverse shapes, textures, compositions, and properties.

3.1. Sol–gel technique

The sol–gel method is one of the most widely used, efficient and versatile methods for producing nanoceramics in various shapes depending on the hydrolysis and condensation processes. It is important to note that the qualities of nanoceramics are determined by particle size, surface, and morphology. On the other hand, Sol–gel is well suited for managing the features mentioned above of nanoceramics. Several studies have reported synthesizing nanoceramics using the sol–gel technique.[41,42] Aydin *et al.* synthesized undoped and Fe-doped SnO_2 nanopowders. Tin(II) chloride was used as the base material, Iron(III) chloride hexahydrate acted as the dopant source, while

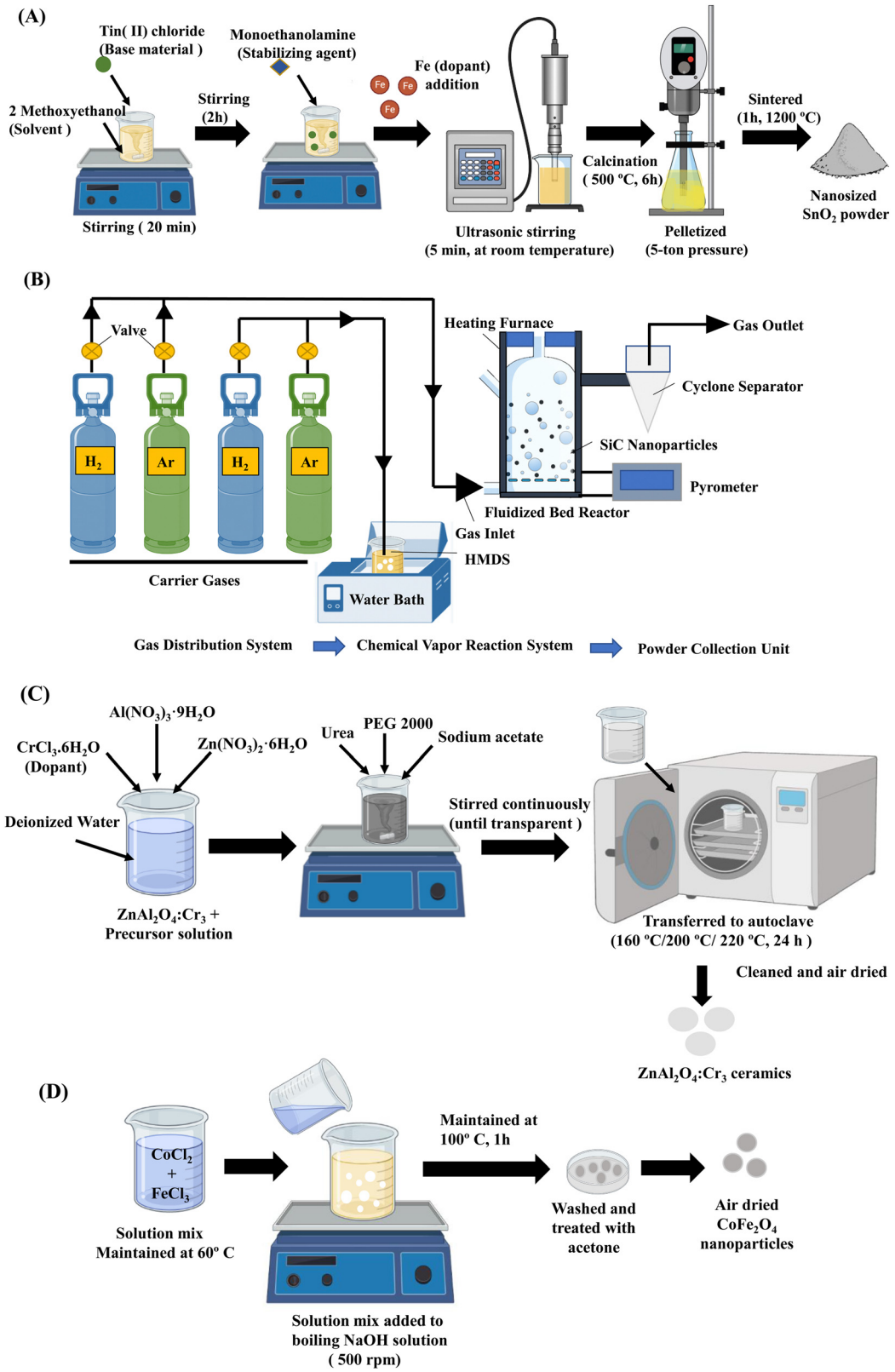

Fig. 3 Synthesis methods of nanobioceramics. (A) Schematic illustration of Fe-doped SnO_2 nanopowder prepared by the sol–gel technique.[42] (B) Synthesis of SiC nanoparticles by fluidized bed chemical vapor deposition method.[43] (C) Preparation of $ZnAl_2O_4$:Cr_3 ceramics by solvothermal method.[45] (D) Chemical precipitation of $CoFe_2O_4$ nanoparticles.[46]

2-methoxy ethanol and monoethanolamine were the solvent and stabilizer, respectively. The nanopowders of SnO_2 were obtained due to calcination and sintering and this ageing process is schematized in Fig. 2A.[42] The techniques such as XRD, SEM, TEM, and energy dispersive spectrometry (EDS) were used to characterize the synthesized nanoparticles.

3.2. Chemical vapor deposition

Chemical vapour deposition is a widely reported method for the synthesis of nanoceramics as well as the production of bulk ceramics. This method involves a precursor that is converted into nanoceramics in the presence of a catalyst at a suitable temperature. Amongst several types of nanoceramics, this method is primarily used to fabricate oxides, nitrides, and carbides. Liu *et al.* used the fluidized bed chemical vapour deposition system that consists of three main parts, namely the gas distribution system, the fluidized bed chemical vapour reaction system and the powder collection system to synthesize silicon carbide (SiC) nanoparticles with adjustable size, stoichiometric ratio, and properties (Fig. 2B). Firstly, the precursor was heated, and the steam was entrained into the furnace using a carrier gas. Secondly, the inflowing precursor gas into the furnace was heated rapidly by hot fluidized particles and finally decomposed at a high temperature. The synthesized nanoparticles were then collected by the cyclone separator.[43] This method of preparation of nanoceramics allows tailoring the particle size by controlling the temperature and gas ratio.

3.3. Solvothermal method

The solvothermal method is widely used to fabricate nanoceramics and typically has a two-step synthesis process, namely chemical mixing and calcination. The advantages of this method include obtaining the final product at a relatively lower reaction temperature and the absence of post-annealing. Also, crystalline materials with different compositions, sizes, structures, and morphology could be prepared by controlling the experimental temperature, pH, and reaction concentration.[44] Zhang *et al.* synthesised $ZnAl_2O_4$:Cr^{3+} nanocrystals by solvothermal method (Fig. 2C). The nanoceramic crystals were of spherical morphology with a diameter of about 500 nm.[45] However, this method carries limitations such as poor dispersion of the nanoceramics and large particle sizes.

3.4. Chemical precipitation

Chemical precipitation is a simple and versatile method of synthesising nanoceramics at an industrially scalable yielding.[46] The precipitation method dramatically depends on the pH of the system. Also, by controlling the rate of nucleation and growth during the processing, the required nanoceramic size, morphology, and particle size distribution can be achieved.[44] There are three types of chemical precipitation: direct precipitation, coprecipitation, and homogeneous precipitation. Amongst these, coprecipitation is the most reported. Safi *et al.* synthesised $CoFe_2O_4$ nanoceramics by coprecipitation method at 60 °C (Fig. 2D). The yielded nanoceramics were highly crystalline with a crystallinity index of 83% and crystallite size of 15 nm.[46] Hence, these methods could produce different nanoceramics of varying compositions, shapes, and properties.

4. Chitosan – a promising biomaterial in tissue engineering

Chitosan is a deacylated form of chitin, a marine-derived polysaccharide that acts as a structural component of crustacean exoskeletons.[47] CS is soluble in dilute aqueous acidic solutions (pH < 6.5) and insoluble in water, organic solvents, and alkaline medium due to the presence of a primary amino group in its structure, which gets protonated and becomes polyelectrolyte in aqueous acidic medium.[48] CS is a linear polysaccharide composed of D-glucosamine and *N*-acetyl glucosamine units linked by β-1,4 glycosidic bonds.[49] CS is known for its diverse applications in numerous biological activities, including antioxidant, anti-inflammatory, antitumoral, and antibacterial effects.[50] Chitin can be converted to CS either by chemical or enzymatic methods, and both the former and latter processes are based on demineralisation, deproteinization, and deacetylation of chitin. The process of deacetylation involves the removal of acetyl groups from the molecular chain of chitin, leaving behind a complete amino group ($-NH_2$) to form CS. CS production through lactic acid fermentation of chitin, employing specific *Lactobacillus* strains, has also been reported.[51]

Knidri *et al.* has demonstrated a faster, easier, and more efficient way to prepare CS from chitin *via* microwave irradiation. The deacetylation method and the degree of deacetylation utilised for CS synthesis play a critical role in determining the polymer chain's composition, size, properties, and application.[52] The degree of deacetylation represents the proportion of D-glucosamine and *N*-acetyl-D-glucosamine[53] and generally falls between 50–95%. It dramatically impacts the solubility, degradation, crystallinity, surface tension, and molecular weight of CS. CS with intermediate degrees of deacetylation is semi-crystalline[54] and favors substantial intra/inter molecular hydrogen bonding. Higher levels of deacetylation are correlated with a higher percentage of positively charged primary amines,[55] resulting in an overall higher charge density. This cationic nature is crucial in BTE applications as CS can form polyelectrolyte complexes with anionic biological macromolecules and DNA.[56] The higher deacetylation degree lowers the material degradation properties of the CS scaffold. Under *in vivo* conditions, CS degradation occurs *via* the action of an enzyme called lysozyme, giving rise to CS oligosaccharides.[57] The degradation rates can be tuned according to the targeted bone defect and ingrowth levels. The suitable degree of deacetylation also varies accordingly. As mentioned earlier, the structural similarity in the chemical structure of CS with glycosaminoglycans, the significant component of the ECM of bone, had made it attractive as a bone scaffold material.

Compared to chitin, CS is more biocompatible and has tailorable properties.[58] Previous studies reported that CS causes only a minimal foreign-body response compared to other natural and synthetic polymers.[57] Additionally, CS offers a

hydrophilic surface that encourages cell attachment and the growth of bone-forming osteoblast cells. Free CS[59] and certain derivatives of CS, including carboxymethyl CS,[60] methyl pyrrolidone[61] have been reported to be capable of inducing osteogenesis both *in vitro* and *in vivo.* Apart from all other advantages and crucial properties, CS has facile fabrication and mild synthesis requirements. It can be synergistically combined with other biomaterials, and can be prepared in various forms, including electrospun nanofibers, hydrogel, nanoparticles, and porous 3D scaffolds. Electrospinning is a relatively simple, emerging, and widely used fabrication technique for creating fibrous bone scaffolds. Interestingly several reports on nanoceramics-loaded electrospun chitosan matrices are available for bone regeneration applications. For instance, Hokmabad *et al.* developed poly(ε-caprolactone)-poly(ethylene glycol)-poly(ε-caprolactone)-CS nanofibers incorporated with nanoceramics such as nHAp and silicon dioxide nanoparticles. The nanofibrous scaffolds demonstrated enhanced mechanical strength, cell adhesion, and subsequent differentiation of human dental pulp stem cells by adding nHAp than silicon dioxide nanoparticles.[62]

The presence of reactive primary amines, primary and secondary hydroxyl groups and side groups on CS makes it possible to add peptides, amino acids, or side groups, enabling CS to be easily functionalised.[63] Therefore, CS has numerous properties make it a promising biomaterial for BTE applications. However, there are a few drawbacks regarding the level of bioactivity and mechanical strength. These can be overcome by combining CS with other materials such as polyglycolic acid (PGA),[64] polyethylene glycol (PEG),[65] ceramics and metals to withstand the *in vivo* stress during bone regeneration.

5. Nanoceramics-reinforced chitosan scaffolds in bone tissue engineering

The CS polymer has desirable qualities for use in the construction of different human tissues, the healing of wounds, and the administration of drugs. It has good adsorption, antibacterial, and nonantigenic capabilities, as well as it does not cause an immunological response and is biodegradable. Another major advantage is that CS is tailorable into several shapes and forms, including gels, nanoparticles, nanofibers, beads, and scaffolds. CS scaffolds could be fabricated with high degree of interconnected, gradient porosity. It has been reported that CS-based scaffolds are osteoconductive and improve bone formation *in vitro* and *in vivo* for BTE purposes.[66] However, to over the limitation of its poor mechanical property, various nanoceramics-based CS scaffolds have been fabricated, which are briefly discussed in the following sections.

5.1. Bioinert nanoceramics reinforced chitosan scaffolds

Bioinert ceramics are completely oxidized materials and therefore exhibit high chemical stability. They often exhibit excellent mechanical and chemical stability *in vivo*. When inserted into living bone, they undergo ''contact osteogenesis,'' which is the process by which they become a part of the bone tissue. Bioinert materials have minimal biological interactions with the surrounding tissue and do not elicit any immunological responses against the graft. These materials possess high tensile strength and toughness, which makes them an ideal candidate for use in BTE practices.[67] However, over time, these materials require secondary surgery and may cause inflammation in the surrounding tissues and release harmful and toxic ions.[68]

Nanomaterials are at the forefront of bone regeneration and tissue engineering in general. Due to their nanoscale dimensions, nanoparticles exhibit greater availability in biological systems.[69] They include nanospheres, nanowires, nanofilms, nanotubes, and many more. The nanoscale reduction in material size dramatically increases surface area, roughness, and the ratio of surface area to volume, resulting in enhanced physiochemical characteristics.[70] Nanoceramics is an organic solid made up of metal or non-metal composition and are a class of advanced ceramic materials having structural dimensions between 1–100 nm.[71] Various bioinert nanoceramics-reinforced CS scaffolds reported to treat intrinsic bone defects have been summarized in Table 1.

5.1.1. Titanium oxide. Titanium is the material of choice for the vast majority of bone defect treatment owing to its excellent biocompatibility, high strength, low density, high corrosion resistance, complete inertness to the body's environment, enhanced compatibility, low Young's modulus, high ability to fuse with bone or other tissues, and formation of a thin surface oxide layer, which makes it an ideal candidate as hard tissue substitutes in artificial bones and joints.[80] Titanium di-oxide nanoparticles have been used as photocatalysts in solar cells, pigment in paints and corrosion-protective coating in bone implants. Ferin *et al.* reported that ultrafine TiO_2 (~20 nm) accessed the pulmonary interstitium in rat lungs and caused an inflammatory response compared with fine TiO_2 at the same mass burden.[81] Ren *et al.* evaluated the effect of different shapes and sizes of TiO_2 nanoparticles on the proliferation and differentiation of MC3T3-E1 (mouse preosteoblastic) cells. The results from the alizarin red staining indicated the formation of mineralized nodules. However, flow cytometry analysis revealed the induction of oxidative stress to MC3T3-E1 cells in response to TiO_2 nanoparticles.[82] Therefore, there are concerns about the biological toxicity of TiO_2 nanoparticles.

Valencia-Llano *et al.* incorporated graphene oxide nanosheets, titanium dioxide nanoparticles, and blackberry processing waste extract on to CS beads and evaluated them as partial bone substitutes (Fig. 4). Synthesis of TiO_2 nanoparticles was done by hydrolysis and peptization of titanium isopropoxide solution. The biocomposite beads were tested in rat models of critical size bone defects with defects of 5 mm × 0.8 mm (diameter × deep) in parietal bones. The histology results confirmed the presence of bundles of collagen type I and the presence of newly formed bone tissue. The presence of calcium and phosphorus confirmed the beginning of mineralization, ECM formation and bone matrix maturation.[83]

Table 1 A summary of bioinert nanoceramic-reinforced chitosan scaffolds in bone tissue engineering

Ceramic material	Biomaterial composition	*In vitro*/*in vivo* models	*In vitro*/*in vivo* results	Ref.
Titanium dioxide	Chitosan/nano-TiO_2 sponge	MSCs isolated from mouse bone marrow of 3 weeks old male C57BL/6 J mice	• Increased apatite formation was observed. • Increased level of osteocalcin (~2-fold) production was observed, indicating osteoblast differentiation.	72
	Nano-TiO_2 doped chitosan scaffold	—	• Enhanced mechanical properties and increased porosity with a pore volume of 0.0030 cm^3 g^{-1} and pore diameter of 2.86 nm were observed. • Incorporation of nano-TiO_2 exhibited a controlled degradation rate of CS.	73
	CS/graphene oxide/TiO_2 nanoparticles/blackberry waste extract	Three-month-old male Wistar rats	• The animal model post-implantation exhibited a non-inflammatory response and hair regrowth, indicating the biocompatible property of the implant. • At the intraosseous level, a fibrous tissue composed of bundles of type I collagen fibers that seem to continue with the periosteum was observed.	74
Zirconium dioxide	CS/nHAp/nano-zirconium dioxide	Mouse MSCs (C3H10T1/2)	• The scaffolds exhibited improved mechanical properties and controlled degradation due to their crystalline nature. • The biocomposite scaffolds showed enhanced osteoinductive properties, and the addition of bioactive molecules such as miR-590-5p to the scaffolds further increased osteoblast differentiation.	75
	CS/Silicon dioxide/Zirconium nanoparticles	Osteoprogenitor cells from 3 days old neonatal Wister rats	• Increased protein adsorption was observed due to increased surface area. • Incorporation of ceramics led to enhanced apatite formation. • The biocomposite scaffolds exhibited a cyto-friendly nature toward the cells.	76
	CS/Zirconium oxide	MG-63 cells	• The biocomposite scaffolds exhibited superior biocompatibility and hemocompatible properties.	77
Alumina	Poly(3-hydroxybutyrate)-CS/alumina nanowires	MG-63 cells	• The presence of 5% alumina was found to increase fiber diameter (645.2 ± 192 nm). • The biocomposite scaffolds with alumina showed a 10-fold increase in their tensile strength. • The alumina-containing scaffolds showed better cell viability.	78
	Silk/CS/Nano-γ-alumina	Human gingival fibroblast cells	• The biocomposite scaffolds exhibited highly interconnected pores thereby providing better cell adhesion. • The presence of γ-alumina enhanced the diffusion rate of nutrients and waste materials. • A controlled biodegradation due to the presence of γ-alumina was noted. • The scaffolds exhibited an increased proliferation rate and cell viability, indicating their cyto-friendly nature.	79

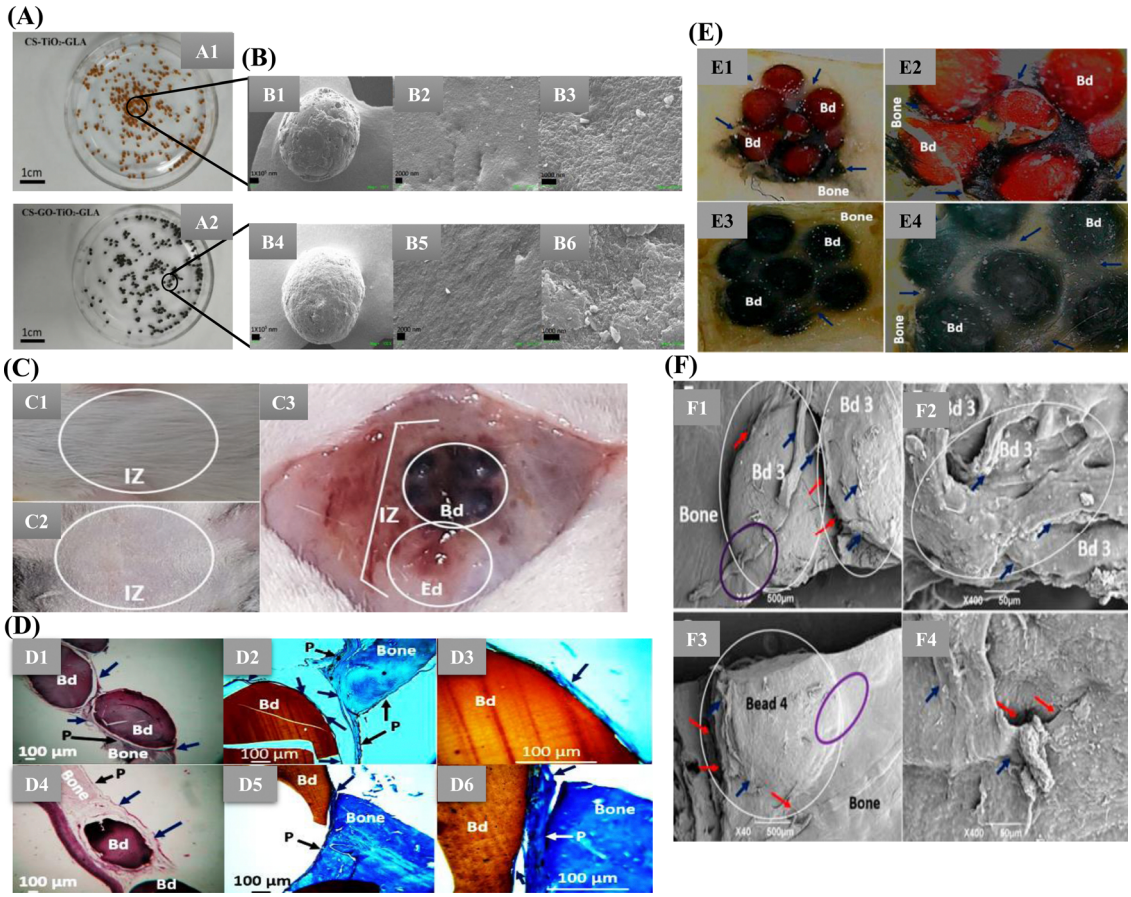

Fig. 4 (A) Images of the different bead composites: (A1) CS-TiO_2-GLA, (A2) CS-GO-TiO_2-GLA. (B) SEM images. Morphology of the beads: CS-TiO_2-GLA (B1) at 100×, (B2) at 1000×, (B3) at 25 000×; CS-TiO_2-GO-GLA (B4) at 100×, (B5) at 1000×, (B6) at 25 000×. (C) Macroscopic image of the skull intervened area. (C1) Presence of hair. (C2) Trichotomy. (C3) Exposed bone area. IZ: implantation zone. Bd: beads. Ed: empty defect. (D) Samples implanted in the cranial bone defect (D1)–(D3) CS-TiO_2-GLA; (D4)–(D6) CS-TiO_2-GO-GLA (D1) and (D4) at 4× H–E technique. (D2) and (D5) at 10× MT technique. (D3, D6) at 40× MT technique. Bd: bead. Black arrow P: periosteum. Blue arrow: soft tissue that covers the beads. Purple oval: Areas where there is continuity of bone-bead soft tissue. White circle: Area of new bone formation. (E) Cranial implantation areas. (E1) CS-TiO_2-GLA at 1×. (E2) CS-TiO_2-GLA at 3×. (E3) CS-GO-TiO_2-GLA at 1×. (E4) CS-GO-TiO_2-GLA at 3×. Bd: Bead. Blue arrows: Soft tissue surrounding intervened areas. Stereoscopic microscope technique. (F) SEM analysis of the cranial implantation areas. (F1) and (F2) CS-TiO_2-GLA. (F3) and (F4): CS-GO-TiO_2-GLA. White circle: Bead implantation area. Red arrow: Interface area bead–bead, bead–bone. Blue arrow: cover soft tissue. Purple oval: Incorporation area of the bead covering soft tissue with the bone covering soft tissue (Open access article under Creative Commons Attribution[83]).

Similarly, Hashemi *et al.* demonstrated metformin's comparative drug release profile loaded onto TiO_2 nanotubes with and without CS film. The CS-coated TiO_2 nanotubes with 15 layers of CS coating showed sustained drug release for up to 21 days. In contrast, the seven layers of CS-coated TiO_2 nanotubes showed seven days of sustained release. This could be attributed to the restriction by polymer chain swelling. The non-coated TiO_2 nanotubes exhibited burst release of the drug. The results also revealed the osteogenic potential of loading Metformin into TiO_2 nanotube arrays and then coating them with CS might increase mesenchymal stem cell (MSC) adhesion, differentiation, and proliferation. Furthermore, a considerable increase in alkaline phosphatase (ALP) activity and collagen I synthesis of TiO_2 nanotubes coated with CS were also observed.[84]

The antibacterial property of TiO_2 nanoparticles was reported by Kolathupalayam Shanmugam *et al.*, who fabricated the CS-alginate scaffold incorporated with TiO_2 nanoparticles by the solvent casting method. The results are promising with the maximum zone of inhibition against *Staphylococcus aureus*. It might be due to the peroxidation of the phospholipids of the bacterial cell membrane, cell wall damage caused by electrostatic repulsions, and respiratory inhibition. CS may also contribute to this bactericidal effect by interacting with the opposing bacterial cell wall.[85]

Yin *et al.* studied the immunomodulatory response of multilayers of CS/alginate films over the Titania nanotubes. The biocomposite films containing Titania nanotubes were studied *in vitro* using bone marrow mesenchymal stem cells (BMSC) to determine their osteogenic effects and regulatory mechanisms. The osteogenic gene expression of BMSCs was upregulated, and biomineralization was stimulated more by alginate/CS multilayer-coated titania nanotube samples than free titania nanotubes. M1 and M2 macrophage polarisation generated by

the substance improved the early and intermediate stages of BMSCs' osteogenesis *via* separate mechanisms: the TGF-β/Smads pathway was activated by M2, whilst M1 activated the BMP6/Smads and Wnt10b/-catenin pathways. Interestingly, research on the rat bone defect model showed that IL-4-loaded immunomodulatory implants could induce a phenotypic macrophage switch from the pro-inflammatory M1 to the anti-inflammatory M2 state, enhancing new bone production.[86] Therefore, titanium oxide incorporated CS biocomposite could reduce post-operative infections attributed to their controllable drug release profile, osseointegration and sustained antibacterial potency. It is becoming clear that macrophages are crucial to the success of biomaterial-mediated osteogenesis. Nevertheless, the precise function of macrophages and the molecular processes by which material characteristics regulate osteogenesis remain unknown.

5.1.2. Alumina. Alumina or aluminium oxide, an aluminium derivative, has also been considered for use in dental and orthopaedic applications because of its favourable mechanical and biological qualities. Monolithic alumina, because of its bioinert nature, does not encourage osseointegration, thus, leading to implant failure. Anodization creates porous ceramic coatings to circumvent this problem.[87] The implant's nanoscale topography and hydrophilicity could support improved adherence of proteins, leading to an upsurge in the production of molecules like vitronectin and fibronectin.[88] Previously, it has been reported that the pore size of the scaffolds could influence cellular behaviour both at the proliferation and differentiation stages. Hadjicharalambous *et al.* reported the effect of porosity on pre-osteoblastic cell attachment and proliferation on alumina and zirconia scaffolds. They inferred that porosity of 49% aided better cell attachment and proliferation.[89]

Teimouri *et al.* studied the silk fibroin/CS/Nano γ-alumina (SF/CS/*n*-γ-alumina) composite scaffolds, which were prepared by lyophilization. Adding *n*-γ-alumina onto these scaffolds led to enhanced compressive strength and better water uptake capacity. However, it led to decreased porosity. The cytocompatibility results showed no signs of toxicity. The presence of *n*-γ-alumina in the SF/CS scaffolds led to better cell attachment and met the requirements for tissue engineering applications.[90] Similarly, Toloue *et al.* reported that adding alumina nanofibers in poly(3-hydroxybutyrate)-CS scaffold prepared *via* electrospinning method enhanced the proliferation and cell viability of the MG-63 (human osteoblastic) cells, increased ALP activity, and calcium phosphate deposits were observed.[91] Therefore, nano alumina's high hardness and abrasion resistance properties could aid in composite scaffold fabrication for BTE applications.

5.1.3. Zirconia. Zirconia, a metal oxide of zirconium, has emerged as a versatile material of interest in implant orthopaedics and dentistry due to its novel properties like high chemical stability, high fracture toughness, bending strength, and biocompatibility. Zirconia-based implants were presented as an alternative to titanium implants. Because of its mechanical qualities, and biocompatibility, zirconia is an appropriate implant material. The osseointegration property of zirconia has been previously reported by Depprich *et al.*, who compared the osseous healing of acid-etched zirconia implants with the titanium in the tibial region of the minipigs. Acid-etching was performed to demonstrate the structured surface modification at the microtopographic, submicrometric, and nanometric levels. This surface modification was necessary for better cell–cell communication, cell adhesion, and cell signalling for the initial osseointegration of the implants. One-week post-implantation, there was a characteristic visible gap between the implant and bone filled with matrix regeneration tissue. After four weeks of implantation, the results indicated woven bone, and after the 12th week, lamellar bone was observed in contact with the implant surface.[92] Under physiological conditions, Yttria stabilized zirconia undergoes a crystallographic phase change from a tetragonal phase to a monoclinic phase, thereby increasing the implant's physical toughness. However, significant phase transformation causes surface roughening, leading to implant cracks. Implant cracks could also happen due to the ageing of the implant, the surface topography of the implant, design and composition, area of the bone defect and biomaterial durability.[93]

Jayakumar *et al.* fabricated chitin-CS with nano-zirconia by lyophilization technique. The SEM analysis revealed that adding nano-zirconia to the chitin-CS scaffold provided an ideal pore size of 150–200 μm for tissue engineering applications compared to the free chitin-CS scaffold with a 200–300 μm pore size. The swelling behaviour showed that adding nano-zirconia aids in the controlled swelling rate as required for the tissue construct. The *in vitro* biomineralization studies showed the apatite formation with a corresponding sharp XRD peak at 32.6° (2θ) of HAp. Cell viability and cell attachment experiments demonstrated that these scaffolds are non-toxic and promote cell adhesion. Therefore, these findings implied that the nanocomposite scaffolds containing nano-zirconia may aid BTE applications.[94]

Alternatively, Balaganagadharan *et al.* reported the osteoinductive property of CS/nanohydroxyapatite (nHAp) biocomposite scaffold containing the nano-zirconia and bioactive molecule miR-590-5p. The biocomposite scaffold enhanced the differentiation of MSCs to osteoblastic lineage at the cellular level. This study suggested that the combination of miR-590-5p and the biocomposite scaffold containing nano-zirconia aids in osteoblast differentiation owing to the activation of several osteogenic signalling pathways.[95]

5.2. Bioactive nanoceramics-reinforced chitosan scaffolds

Bioactive nanoceramics are ceramics that possess enhanced osteointegrative and osteoinductive functions contributed by their topographical features and surface chemistry. They include several types of bioactive glass nanoceramics that could be readily absorbed by the cells. Despite the bioactive ceramics' unique biological interaction with bone tissue, they may only meet some clinical applications since ceramic materials' mechanical properties differ from those of natural bone. In light of this, the novel bone-repairing biocomposite materials with improved bioactivity and mechanical capabilities would result from combining bioactive nanoceramics with preferably CS.[57] Table 2 summaries various bioactive nanoceramics-reinforced CS scaffolds in BTE.

Table 2 A summary of bioactive nanoceramic-reinforced chitosan scaffolds in bone tissue engineering

S. no.	Scaffolds/composites	*In vitro* analysis	*In vivo* model systems	*In vivo* analysis	Ref.
1	Human amniotic fluid-derived stem cells (hAF-MSCs) incorporated in 30% nHAp/CS scaffolds	High proliferative and osteogenic potential of hAF-MSCs were observed.	New Zealand White rabbit; tibial defect diameter-0.5 mm and depth-0.5 mm	• At 2–3 weeks post-surgery, the *in vivo* model showed a new bone formation at the defect site and complete bone healing at the end of the 4th week.	96
2	Injectable thermosensitive zinc-doped CS/nHAp/β-glycerophosphate hydrogels	The biocomposite hydrogels showed enhanced swelling, protein adsorption, and exogenous biomineralization and osteogenic potential.	Male Wistar rat; right tibial defect	• Apatite and collagen deposits were observed, indicating accelerated bone formation at 2 weeks post-transplantation.	97
3	Human gingival fibroblasts seeded on sphere-shaped nHAp/CS/Gel 3D porous scaffolds	Increased osteogenic differentiation was noted.	Male immunocompromised mice; 4–10 mm defect in the right hind leg	• At 12 weeks, bone formation was observed.	98
4	CS/nHAp scaffolds	Increased cell proliferation of MC-3T3-E1 cells upon the scaffolds was observed.	New Zealand white rabbit; tibial defect	• An increase in bone morphometric parameters was reported at 8 weeks post-transplantation.	99
5	Silk fibroin/CS/nHAp scaffolds	Biocompatibility and increased osteogenic potential were reported.	New Zealand white rabbit; 2 cm right radial bone defect	• New bone formation at 16 weeks post-surgery indicating the osteoinductive and osteogenic effect of scaffolds.	100
6	PLA/nHAp/alendronate loaded CS microspheres	The sustained release of the drug from the biocomposite scaffolds was noted. The biocomposite scaffold showed an enhanced osteogenic differentiation of adipose-derived stem cells.	New Zealand white rabbit; 1.5 cm segmental bone defect created on the bilateral radius	• A complete bone healing at 8 weeks post-implantation was observed.	101
7	Anisotropic spiral-cylindrical CS/cellulose/nHAp composite scaffolds	Enhanced cell attachment, migration, proliferation, and differentiation of osteoblasts were observed.	New Zealand white rabbit; concave defect at the middle segment of the left radius with length-10 mm and depth-3 mm	• Osseointegration and functional reconstruction of bone defects were observed. • The biocomposite exhibited new bone formation at 12 weeks post-surgery.	102
8	BMSCs loaded on silk fibroin/CS/nHAp scaffolds	Enhanced biocompatible and biodegradable properties were seen. Increased cellular adhesion, growth, calcium nodule formation, and osteogenic differentiation of BMSCs, thereby promoting new bone formation, was observed.	New Zealand White rabbit; 15 mm segmental defect in the radius	• Gradual new bone formation and bone defect recovery at 12 weeks were noted.	103
9	Silk fibroin/CS/nHAp composite scaffolds in combination with autologous concentrated growth factor	Enhanced proliferation and osteogenic differentiation of BMSCs on the biocomposite scaffold were noted.	New Zealand white rabbit; a cylindrical bone defect created in the middle of the radius with length-15 mm and diameter-3 mm	• Significant increase in collagen formation and mineralization was reported. Improved the repair efficiency of critical bone defects at 12 weeks.	104
10	PTH-derived peptide-loaded nHAp/CS coated true bone ceramics	A sustained release of PTHdP from the scaffolds was observed.	New Zealand white rabbit; 15 mm critical size radial defect	• The results showed excellent biocompatibility and osteoconductive capabilities for the targeted bone-implant integration, and subsequent new bone ingrowth at 12 weeks post-surgery.	105

5.2.1. 45S5 Bioglass. Bioactive glasses (BG) nanoceramics are biodegradable and osteogenesis-promoting biomaterials used to repair injured bone. The BG was invented by Professor. Larry Hench at the University of Florida in 1969.[106] BG 45S5 is often applied in the orthopedic and dental fields, where it promotes the body's natural bone healing[107] by providing calcium (Ca^{2+}) and phosphate (PO_4^{3-}) ions to create hydroxycarbonate apatite, the main mineral component of animal bone tissue.[108] Due to the above-mentioned characteristic features and its excellent ability as a carrier of cells, BG 45S5 is currently one of the most reported biomaterials in BTE applications. BG 45S5 has superior mechanical qualities due to its composition containing several phases and enhanced solubility in body fluid than ceramics. As a result, it was suggested that bioactive glass ceramics can be created with mechanical characteristics that are considerably more similar to those of natural bone.[109] The traditional preparation of BG by crystallization and melting technique has a downside of the evaporation of volatile components during high-temperature processing. Therefore, sol–gel technique is widely used to overcome high-temperature evaporation limitations of conventional techniques as it also permits the fabrication of various BG compositions with high uniformity, purity, and forms, such as monoliths, powders, fibres, and coatings.[110] Furthermore, the glass-ceramics produced by this method have more significant surface areas and porosities, which are crucial for their bioactivity.[111]

Due to its excellent mechanical strength, BG can be used as reinforcement in other materials like naturally occurring polymers, which enhances its properties and allows for the most effective use.[112] CS is recently gaining popularity as an effective polymer for class II hybrid scaffolds with BG. CS was functionalized with 3-glycidyloxypropyl trimethoxysilane (GPTMS) using sol–gel synthesis to produce covalent interactions with BG.[113] BG is commonly used in combination with electrophoretic deposition to develop bioactive coating. Various studies have shown that including CS and its derivatives in composite coatings increases biocompatibility and protects metallic implants against corrosion.[114,115]

Parvizifard and Karbasi investigated the results of poly-(3-hydroxybutyrate) (PHB)-CS/multi-walled carbon nanotubes (MWCNTs) nanocomposite coating deposited on nano-BG-based scaffolds. The results revealed that scaffolds had a high proportion of interconnected porosity and upon comparing the scaffolds with and without the PHB-CS/MWCNTs coating to nano-BG scaffold, the compressive strength of the scaffold having a coating increased up to 30 times. The SEM, EDAX, and XRD results indicated that the presence of PHB-CS/MWCNTs increased the apatite-like formation. In addition, PHB-CS/MWCNTs nanocomposite coating increased MG-63 cell survival, proliferation, and ALP secretion.[116] Therefore, BG has been reinforced and used as nanofillers resulting in enhanced osteogenic activity as indicated by increased level of ALP. Elevated ALP is a sign that active bone production may occur because ALP is a consequence of osteoblast activity.[117]

5.2.2. Hydroxyapatite. nHAp crystallizes in hexagonal form and belongs to the apatite family. The general formula of calcium apatites is $Ca_5(PO_4)_3X$, where X denotes the Halide ion or OH group. The important calcium apatites are HAp, fluorapatite (FA) and chlorapatite (CA). The apatite structure can also be substituted by ions such as Sr^{2+}, Pb^{2+}, Cd^{2+}, Mn^{2+}, *etc.*, at Ca position which results in changes in the properties. Advancements in medical science and surgical techniques have led to the use of synthetic HAp as a biomaterial for bone implants. Amongst all the bioactive nanoceramics, nHAp is the most appropriate choice for bone scaffolds as it directly binds to the bone and shows excellent biocompatibility and osseointegration. Also, nHAp increases the surface area and porosity of the bone matrix.

Since collagen fibres and nano-sized, needle-like nHAp crystals make up most of the composition of natural bone, a biocomposite scaffold containing nHAp and CS biopolymer would mimic the bone microstructure with exceptional biodegradable and biocompatible properties.[118] In restoration and prevention, nHAp exhibits amazing re-mineralizing effects on critical defects, unquestionably greater than the conventional materials utilized up until now. Also, nHAp is a better source of free calcium that is essential for remineralisation.[119] In a study by Atak *et al.*, three different scaffolds, including a specially modified composite scaffold, were fabricated for osteogenic evaluation. The scaffold was composed of CS, CS/nHAp composite, and an amine group (NH_2) modified nHAp/CS composite (CS/nHAp-NH_2) scaffolds. The findings demonstrated the biocompatibility of all three types of scaffolds, while more specifically CS/nHAp-NH_2 scaffolds supported the greatest amount of cell proliferation in the water-soluble tetrazolium assay and showed the least cytotoxicity in the lactate dehydrogenase test in human bone mesenchymal stem cells.[120] Similarly, Zhang *et al.* reported that self-assembling peptide (SAP) dramatically improved cell adhesion when added to the nHAp/CS scaffolds. The novel SAP/nHAp/CS compound scaffold materials demonstrated much higher mechanical strength without significantly modifying its cytotoxicity or degradation rate. According to the *in vivo* study shown in Fig. 5, newly produced nanocomposites were viable for the repair of femoral condyle injuries. In this aspect, the nHAp/CS composite material outperform other standard scaffolds and are excellent constructs for BTE applications.[121]

5.2.3. Other bioactive nanoceramics. Several other bioactive nanoceramics have been reported to aid bone tissue regeneration, including whitlockite (WH), cerium oxide (CeO), and diopside (Dp) nanoparticles. WH is present along with HAp in the bone collagen matrix and plays a significant role in the early stages of bone development. WH is, therefore, one of the main constituents in human bone tissue, accounting for approximately 25 wt% of the inorganic bone matrix.[122,123] The biocompatibility, osteoinductivity, and bone regeneration properties of WH were evaluated by Xiao *et al.* in rat calvarial defect models. Using a freeze-drying technique, they synthesized gadolinium-doped whitlockite/chitosan (Gd-WH/CS) composite scaffolds. The scaffolds had a well-interconnected porous architecture with pore sizes ranging between 150–300 μm. The *in vitro* and *in vivo* studies revealed the osteogenic potential of

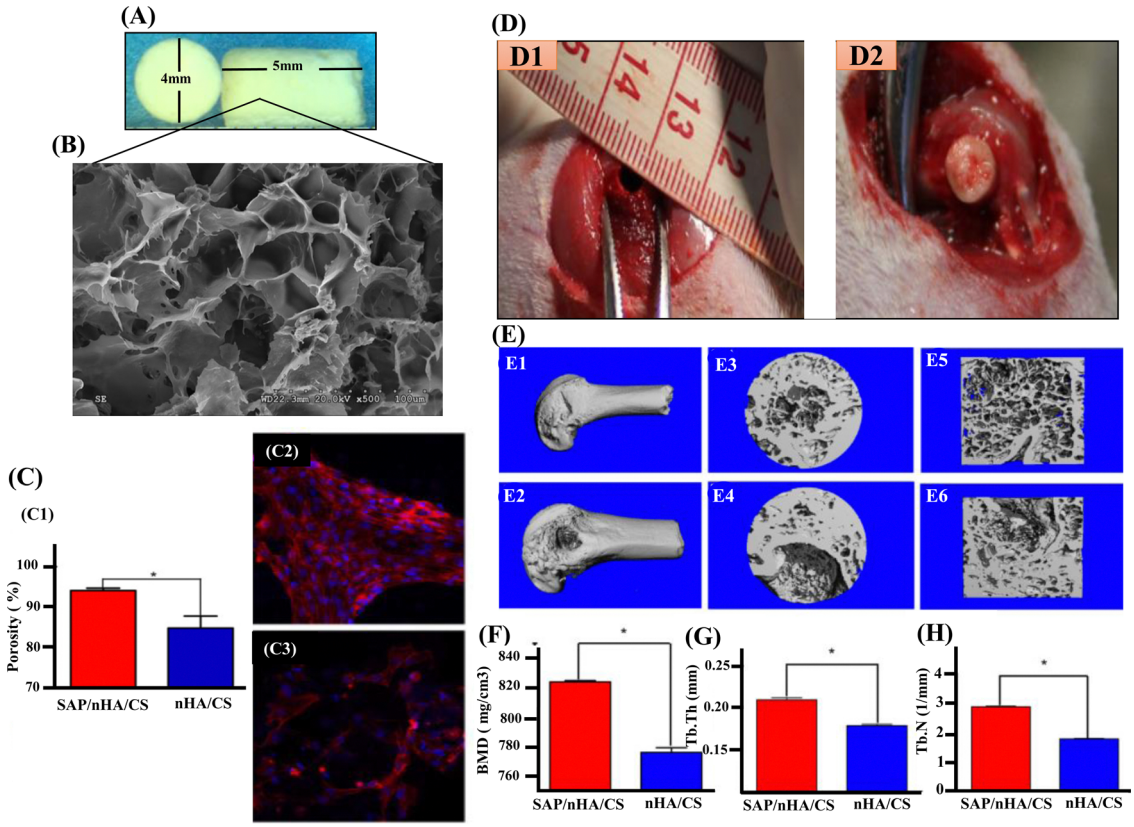

Fig. 5 (A) and (B) The morphology and SEM of SAP/nHA/CTS. (C) and (C1) The percentage of BMSC attachment on scaffolds. SAP/nHA/CTS scaffolds showed higher cell attachment capabilities 94.1% ratio than that of nHA/CTS scaffolds, 84.9%. * Shows significant difference between SAP/nHA/CTS and nHA/CTS, ($p < 0.05$). (C2) The cells on SAP/nHA/CTS scaffolds. (C3) The cells on nHA/CTS scaffolds. (D1) Critical-sized bone defect (4 mm in diameter) was created in the middle of femoral condyle in rat. (D2) BMSCs/nHAp/CTS (or BMSCs/SAP/nHAp/CTS) scaffolds were implanted into the defect area. (E1) and (E2) Only a small portion of the bone defect was not repaired in BMSC/SAP/nHAp/CTS group (E1), meanwhile a large number of bone trabeculae existed in the coronal surface of the bone defect area in BMSC/nHAp/CTS group (E2). (E3) and (E4) in 3D reconstruction of bone defect areas, there were still large bone defect areas. (E5) and (E6) Section diagram of E3 and E4, respectively (F) bone mineral density (BMD) (G) trabecular bone number (TB.N) and (H) trabecular bone thickness (Tb.Th) within the defect were measured by μCT. * indicates that the groups are significantly different from one another ($p < 0.05$). Reproduced with permission.[121] Copyrights 2018, Materials Science & Engineering C.

Gd-WH/CS composite scaffolds *via* the GSK3β/β-catenin signaling pathway. Therefore, these composite scaffolds could be used as bone tissue substitutes in clinical trials.[124]

CeO nanoparticles or nano-ceria have recently drawn significant interest in BTE.[125] Several studies have demonstrated ceria's osseointegration, osteogenic and antibacterial properties.[126–128] For instance, Yildizbakan *et al.* have fabricated the CS-CeO porous scaffolds for the controlled release of antibacterial agents to treat infections associated with bone trauma. The study used increasing concentrations of the CeO (10, 20, and 30 wt%) in the CS-based bone scaffolds and evaluated its corresponding antibacterial property. The scaffold group containing 30 wt% CeO nanoparticle concentration demonstrated promising maximal antibacterial properties with an estimated 88% reduction in bacterial proliferation.[129] Dp nanoparticles are also widely used as bioactive ceramics in BTE.[130] The release of silicon and magnesium ions from the Dp lattice contributes to Dp nanoparticles' enhanced osteoblast proliferation, differentiation, and bone formation potential.[131] Kumar *et al.* reported the synthesis of CS/Dp scaffolds *via* the sol–gel method and subjected them to various physicochemical and *in vitro* characterizations. The results showed that the CS/Dp porous scaffolds exhibited controlled swelling and enhanced apatite formation. Additionally, the CS/Dp scaffolds' *in vivo* biocompatibility and osteogenic potential make them suitable candidates for BTE applications.[132]

5.3. Bioresorbable nanoceramics-reinforced chitosan scaffolds

Bioresorbable nanoceramics are naturally absorbing materials that the body can break down and absorb without causing any adverse reactions. The most common bioresorbable material in BTE is tricalcium phosphate [TCP; $Ca_3(PO_4)_2$]. Calcium phosphate has been widely used in bone regeneration applications because it shows osteoconductive and, in some cases, osteoinductive features. Table 3 summarizes the reported bioresorbable nanoceramic-reinforced chitosan CS scaffolds in BTE.

A crucial factor in boosting the strength properties of a composite scaffold is the size band (micro or nano) of the ceramic employed as filler material. There have been reports on

Table 3 A summary of bioresorbable nanoceramic-reinforced chitosan scaffolds in bone tissue engineering

Bioresorbable nanoceramics	*In vitro* models	Inferences	Ref.
CS/Gel/dihydrogen calcium phosphate anhydrous (DCPA) biocomposite scaffolds	MG-63 cells	• The scaffolds showed improved cell adhesion, proliferation, and differentiation of pre-osteoblasts into an osteogenic lineage with an increase in DCPA concentration for up to 10 wt%.	133
CaP/CS composite coated titanium substrate	MG-63 cells	• The CaP/CS composites showed better cell viability, adhesion, and differentiation compared to the HAp/CS composites.	134
CS/carboxymethyl cellulose (CMC) reinforced with multiphasic calcium phosphate whisker-like fibers	MG-63 cells	• The formation of a polyelectrolyte complex between CS and CMC resulted in improved mechanical strength of greater than 300% compared to pure CS. • The incorporation of calcium phosphate showed the highest mechanical properties, enhanced cell attachment, proliferation, and mineralization, as a function of the fiber content than pure CS and biphasic calcium phosphate fibers.	135
Gel/CS/nano-β-TCP based scaffolds	Human MSCs	• The prepared scaffolds had highly interconnected pores and porosities larger than 80%. • Increasing β-TCP content into the CS/Gel matrix significantly improved mechanical strength from 1 ± 4.3 to 2.45 ± 1.95 MPa and enhanced protein adsorption. • The maximal concentration of β-TCP exhibited good biocompatibility and promoted better cell proliferation and MSC's differentiation.	136
Freeze-gelled CS/nano-β-TCP scaffolds crosslinked with Genipin	Human MSCs	• The biocomposite scaffolds had interconnected microporous structures with porosity greater than 65%. • With respect to the porous characteristics due to the crosslinking concentration, the compressive strength showed a bimodal effect with increased and decreased compressive strength for lower and higher concentrations, respectively.	137
CS/PCL/nano-β-TCP composite scaffolds	Human MSCs	• There was enhanced compressive strength of the biocomposite scaffolds (5.2 ± 0.38 MPa) at 10 wt% PCL concentration. • With respect to the porous nature, the scaffold with a maximal concentration of PCL showed better cell attachment and spreading onto the porous architecture.	138

how nano-TCP, compared to micro-TCP, imparts superior mechanical strength.[139] Beta tri-calcium phosphate (β-TCP), a crystalline form of calcium phosphate, when compared to HAp, is more osteoconductive and biodegradable, thereby directing rapid absorption and gradual replacement by new bone matrix.[140] The release of calcium and phosphate ions from β-TCP could induce the differentiation of MSCs into osteoblastic lineage by activating intracellular mechanisms. There are studies indicating the Gel/CS/β-TCP scaffolds with improved cytocompatibility for bone tissue engineering applications.[141,142] However, these studies did not address the coherent relationship between synthesis–structure–functional properties of the scaffolds. Also, these studies reported that the Gel/CS scaffolds containing β-TCP particles had a compressive strength below 1 MPa that cannot meet the mechanical strength requirement of a bone scaffold. Maji *et al.* fabricated the Gel/CS/β-TCP (GCT) composite scaffolds with improved compressive mechanical behavior and *in vivo* biocompatibility with a controlled degradation rate to address these challenges. The GCT composite scaffolds were synthesized using the solid–liquid phase separation method, followed by subsequent lyophilization. β-TCP nanoparticles were added into the composite scaffolds for bone tissue regeneration to obtain better mechanical and biological properties (Fig. 6). The results indicated that increasing β-TCP nanoparticles content in the Gel/CS scaffolds significantly improved the compressive strength of the scaffolds. More specifically, the 30 wt% addition of β-TCP nanoparticles resulted in an enhanced compressive strength of 2.45 MPa, which matches the mechanical properties of cancellous bone. *In vivo* studies also showed that the Gel/CS composite scaffolds with 30 wt% addition of β-TCP promoted new blood vessel formation. Therefore, β-TCP nanoparticles are potential candidates for bone tissue regeneration.[140]

Keikhaei *et al.* synthesized β-TCP nanoparticles loaded poly(3-hydroxybutyrate) (PHB)-CS electrospun nanofibrous scaffolds. The results showed that adding different amounts of β-TCP nanoparticles increased fibre diameter, porosity, hydrophilicity, and tensile strength. More specifically, adding 7.5 wt% of β-TCP nanoparticles to the PHB-CS scaffolds resulted in better mechanical strength of 9 MPa with 82% porosity and an average fibre diameter of 780 nm. Also, these scaffolds showed better cell attachment and viability.[143] Therefore, β-TCP nanoparticles are excellent additives to a biocomposite scaffold that would be a desirable option for BTE.

6. Nanoceramics-mediated osteogenic signal transduction pathways

Specific signalling molecules and their family members involved in a cascade of intracellular signalling events leading to osteoblast proliferation and differentiation have emerged as therapeutic targets to cure bone defects effectively. A better understanding of the ligands, growth factors, and genes involved in the signalling pathways, and the enhancement of osteoblast proliferation and differentiation upon upregulation or downregulation of specific

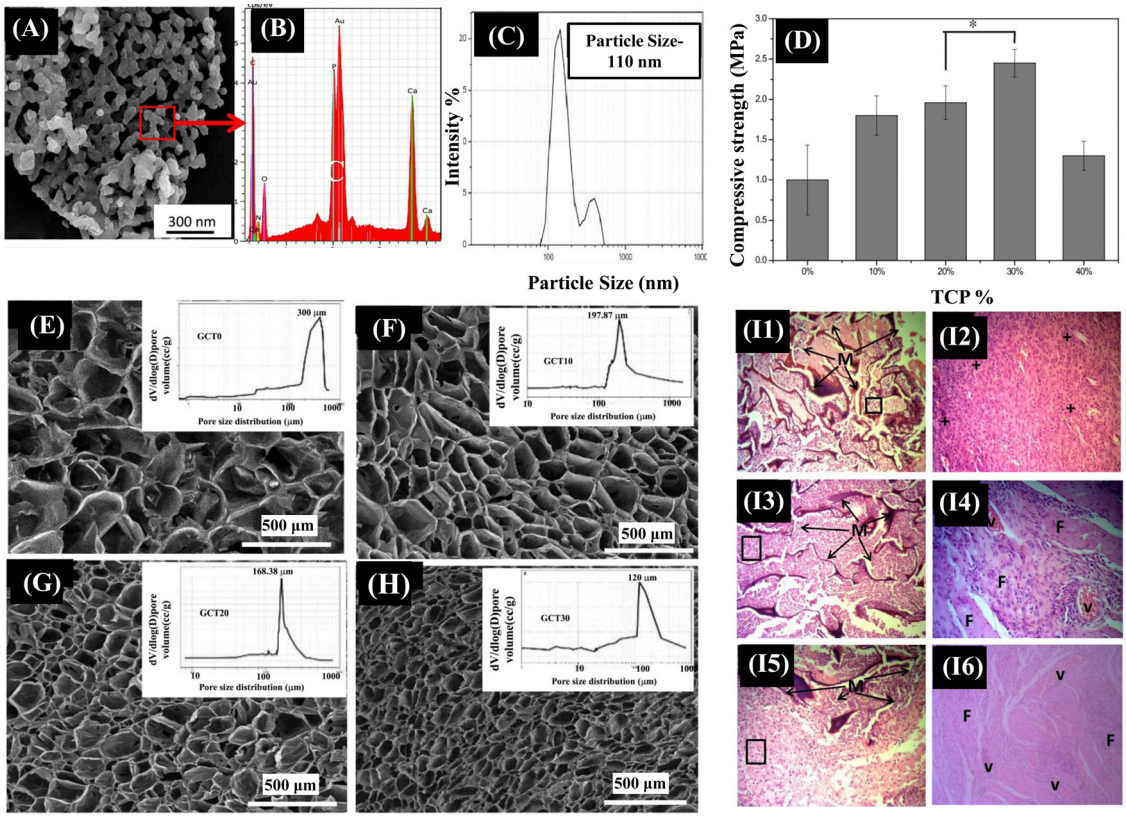

Fig. 6 (A) SEM examination clearly revealed an average particle size of spherical β-TCP particles varying between 70–100 nm, which is corroborated well with the particle size data obtained from DLS measurement (C). (B) Ca/P ratio of as synthesized β-TCP powder was 1.5, as determined using EDX analysis. (D) The mechanical properties obtained from compression tests of both Gel-CS and Gel-CS-β-TCP (GCT) composite scaffolds. (E)–(H) cross-sectional structures of prepared GCT composite scaffolds with varying concentrations of β-TCP. (I1) and (I2) Histologically, after 2 weeks of implantation into mouse skin, the open pore morphology of the scaffold was maintained, but the scaffold integrity was worse. The infiltrating cells began to change into lymphocytes and plasma cells, which was the indication of the first phase of wound healing. (I3) and (I4) At 4th week, cellular infiltration with lymphocytes was decreased with formation of ECM throughout the composite scaffolds. Blood capillaries began to appear in between the almost disintegrated scaffold structure and scaffold interspaces were fully filled with ECM of fibroblasts. (I5) and (I6) At 8th week after implantation, lymphocyte infiltration was further decreased as the vascular structure was prominent inside composite scaffolds. Reproduced with permission.[136] Copyrights 2018, Materials Science & Engineering C.

signaling pathway would provide an insight into the possible treatment options using nanoceramic-reinforced CS scaffolds for bone regeneration. Runx2 (runt-related transcription factor 2) is a bone transcription factor involved in osteoblast differentiation and is essential for the regulation of bone-related proteins *via* several signaling pathways. Osteocalcin (OC), a HAp-binding protein, and ALP, a membrane-bound tetrameric enzyme, are examples of prominent bone turnover markers[144] that are produced by active osteoblasts expressed at different stages of their development and these reflect different aspects of osteoblast function, bone formation, and resorption. An increase in the expression of the bone metabolic markers was found in several studies that used CS as a carrier to deliver biological molecules at the site of the bone defect. Moreover, CS is a well-known biomaterial that has the potential to regulate ECM mineralisation, and it plays an essential part in the maintenance of skeletal homeostasis by stimulating the activity of several different signaling pathways, including Runx2, BMP,[145] and Wnt.[146] Nanoscale bioceramics and CS as the composite scaffolds are highly anticipated to enter clinical studies over the next decade. Major signalling pathways involved in nanoceramics-mediated bone regeneration are summarized as follows.

Bone morphogenetic proteins (BMPs)/Smad,[147] Notch,[148] MAPK, and Wnt are the major signaling pathways regulating osteogenic activity and have been found to regulate the expression of Runx2, an osteogenic marker. BMPs are multifunctional cytokines constituting a significant portion of the TGF-β family of ligands.[149] Initially isolated from demineralised bones, BMPs are known to activate both osteoblasts and osteoclasts through both SMAD-dependent and SMAD-independent signalling and have a unique capability of inducing heterotopic bone formation in skeletal muscle.[150] BMPs play a vital role in the early development of mammals, notably in mesodermal patterning, organ development, and postnatal tissue homeostasis.[151] In a family of more than 20 BMP proteins,[152] every BMP protein plays a significant role in maintaining bone homeostasis.

Interestingly, nanoceramics have been shown to initiate the BMP/Smad pathway in BTE applications. Wang *et al.* fabricated

biphasic calcium phosphate (BCP) and nHAp-coated BCP scaffolds for a comparative study. They confirmed that the latter shows enhanced osteogenic properties under *in vitro* and *in vivo* conditions. The scaffolds were implanted in an intramuscular defect-induced rabbit model. It was reported that nHAp-coated BCP scaffolds favoured cell adhesion and promoted osteogenic differentiation of BMSCs. This was confirmed by the upregulated expression of osteogenic genes, enhanced ALP activity, and increased OCN production. The nHAp-coated BCP-treated group displayed considerably activation of the BMP/Smad signalling pathway. Also, the nHAp-coated BCP scaffolds maintained structural integrity and induced ectopic bone formation.[153] Nanoscale ceramics coupled with CS have also been reported to induce osteoblast differentiation through the BMP/Smad signaling pathway. In another study, Liu *et al.* evaluated the *in vitro* and *in vivo* osteogenic potential of the biomimetic nanocomposite nanofibrous scaffold composed of nHAp/CS seeded with BMSCs. It was reported that nHAp/CS scaffolds showed enhanced bone formation with increased Smad1, BMP-2/4, Runx2, ALP and collagen I mRNA levels. Also, integrin subunits together with myosins were significantly upregulated by nHAp/CS scaffolds confirming nHAp/CS stimulated osteogenic differentiation of BMSCs through the BMP/Smad signalling pathway under both *in vitro* and *in vivo* conditions.[154]

Notch signaling is another pathway regulating skeletogenesis and plays a crucial role in tissue homeostasis, adult stem cell maintenance, chondrogenesis, osteoblastogenesis, and osteoclastogenesis.[155] The Notch family comprises four receptors, namely Notch (1–4) and five traditional DSL (Delta/Serrate/Lag-2) ligands named JAG-1 and 2 (Jagged 1 and 2), DLL (Delta-like 1–4).[156] Abnormal functioning of the Notch signaling pathway results in human skeletal defects such as spondylocostal dysostosis (SCDO),[157] Alagille syndrome, and the Hajdu-Cheney Syndrome.[158] The exact role of the Notch pathway in osteoblast differentiation has not yet been completely reported and remains unclear. Since every cell receives multiple signals simultaneously at the exact moment, it can be understood that the Notch pathway could not express its effect in isolation and would work in coordination with other pathways to induce osteoblast differentiation. Studies have revealed that nanoceramics coupled with CS could initiate osteogenesis through the Notch pathway. For instance, Zou *et al.* reported the cranial bone regeneration capacity of a CS/Alginate hydrogel containing parathyroid hormone (PTH) peptide and nHAp. The biocomposite scaffolds showed excellent biocompatibility and enhanced osteogenic differentiation of rat bone marrow mesenchymal stem cells (rBMSCs) *via* the Notch signaling pathway. There was an upregulated expression of BMP2, Runx2, OC, ALP and osteopontin (OPN).[159] Bioactive and bioinert ceramics like calcium phosphate[160] and titanium,[161] respectively, too can promote osteogenic differentiation *via* the combined effect of the Notch and Wnt signaling pathways. Thus, it can be understood that nanoceramics could modulate bone regeneration *via* a notch signalling pathway.

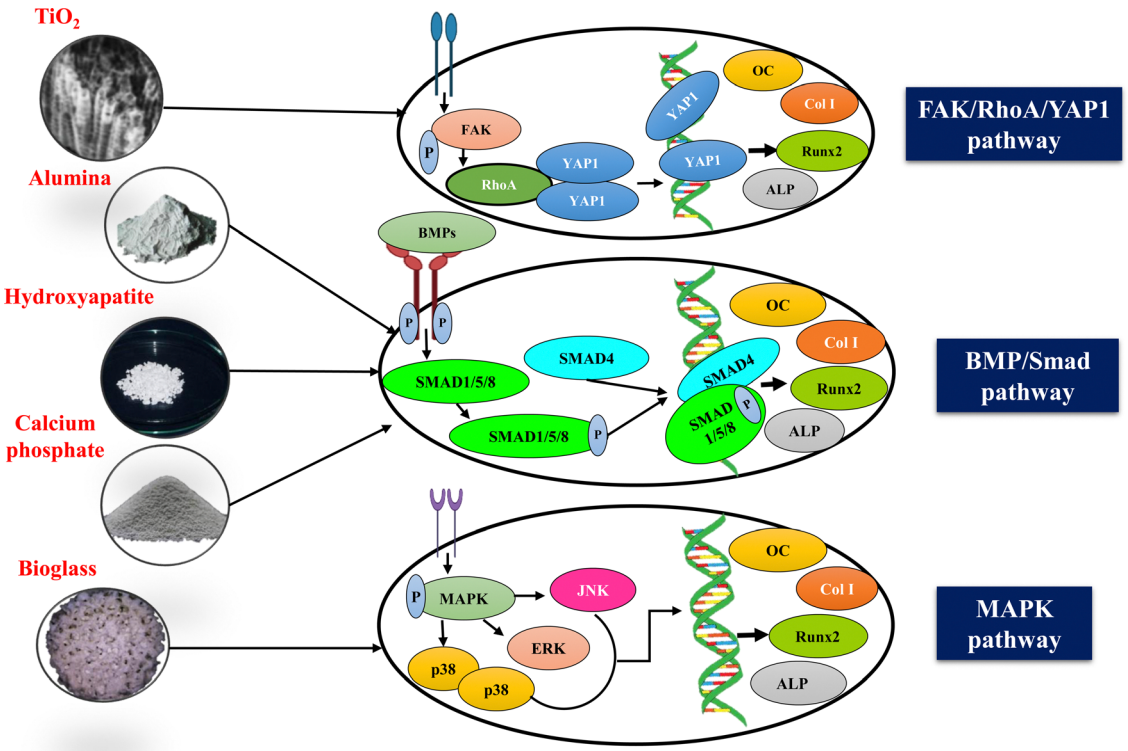

Fig. 7 Schematic illustration of the osteogenic signaling pathways modulated by nanoceramics. The fundamental process of bone regeneration is the induction of osteogenic differentiation, which is only possible through activating specific signaling mechanisms. Nanoceramics-mediated stimulation of these signaling pathways, such as FAK/RhoA/YAP1, TGF-β/BMP, MAPK, and Wnt mechanisms, could activate several transcription factors, including Runx2 and upregulate osteoblast differentiation marker genes, such as OC, type I collagen (COL1) and ALP, leading to enhanced bone regeneration.

Several other signaling pathways have been reported to be involved in the bone repair process mediated by nanoceramics. According to Gong *et al.*, bioactive nano-sized BG particles can enhance the proliferation of MG-63 cells *via* the MAPK pathway,[162] while Zhang *et al.* reported that titanium nanotubes can promote new bone formation through the FAK/RhoA/YAP signaling pathway.[163] Fig. 7 depicts the mechanism of several signalling pathways mediated by nanoceramics. For efficient bone repair, angiogenesis is crucial. Vascularisation helps in promoting osteoclast degradation and aids in the supply of required nutrients like oxygen, osteoblast, and precursors of osteoblasts to the site of the bone defect.[164] Silicate-based nanoceramics, such as bioactive glasses, have been reported to have angiogenic potential.[165] Zhu *et al.* fabricated the Lanthanum-doped mesoporous BG/CS composite scaffolds (La-BGs/CS), and found the elevated expression of angiogenic-related genes of VEGF, b-FGF, and PDGF, thus confirming the angiogenic potential of the synthesised biocomposite scaffold.[166] However, further studies are required to study the synergistic effect of nanoceramics and CS on angiogenesis and osteogenesis.

7. Challenges and future perspectives

In recent years, these nanomaterials have been widely used in orthopaedics owing to their advantages, such as better cellular uptake and adhesion, improved proliferation, and site-specific drug delivery. Nanoceramics-reinforced CS scaffolds can be optimized for a degradation rate matching the new bone formation. FDA-approved bone substitutes include Pro Osteon®, Bioglass®, Collagraft®, and (iv) Grafton®. Bioglass® has been used for long bone fracture fixation, spinal fusion, and joint replacement. FDA-approved nanoceramics include Crystal® Ultra, Zirconia, and GrandioSO. Miniscule alteration in the chemical structure and composition of the nanoceramics can radically alter their properties, playing a role in their toxicity. Toxicity studies on nanoceramics for BTE applications are mandatory due to their insoluble nature in solvents and unique chemical properties. Their high reactivity could disrupt the sample testing as their structural and chemical integrity might alter from synthesis to analysis. Though nanoceramics are innovative materials that perfectly mimic biological systems, they could also intensely affect the treatment scenario due to their high reactivity and toxicity. Therefore, a better understanding of the nanoscale surface topography and interactions between nanoceramics and biological systems is required.

This review mainly focused on the various nanoceramics in conjunction with CS scaffolds to stimulate bone regeneration, vascularisation, and their signalling mechanisms in various *in vitro* and *in vivo* studies. Despite the extensive research on nanoceramics-reinforced CS scaffolds, challenges still need to be addressed before these constructs enter clinical trials. These challenges include toxicity evaluation, degradation, and *in vivo* animal assessments. Investigating how cells interact with nanoscale ceramic structures may shed light on their performance *in vivo*. The loading capacity of drugs and bioactive factors for improving antibacterial effects, vascularisation, gene delivery, and decreasing activity of osteoclasts and other inhibitors can be further increased by optimising the processing parameters and techniques currently used for synthesising the materials. *In vitro* tissue construction under the appropriate growth factors, physicochemical conditions, and pre-designed scaffolds tailored to the individual patient's demands are examples of state-of-the-art techniques that may improve scaffold integration with the host tissue. Integration of the scaffolds with the host tissue may be enhanced by using cutting-edge procedures such as *in vitro* tissue building with optimal growth factors and physicochemical conditions or by using pre-designed scaffolds specifically adapted to each patient's needs. Optimising the material's physical properties may contribute to its increased shelf life and reduced toxicity *in vivo*. In addition, further investigation of the mode of action of these scaffolds using molecular markers and *in vivo* studies is extensively required to study the mechanism of the scaffolds in clinical practices.

8. Conclusions

Nanoceramics are one of the most preferred biomaterials in BTE due to their biocompatibility, enhanced mechanical strength, minimal tissue reaction, and biomimetic nature similar to the mineral composition of the bone. Also, CS-based scaffolds have gained tremendous interest in tissue engineering. Thus, in this review, we overviewed nanoceramics' scientific results on utilizing cutting-edge CS-based nanoceramics in tissue engineering, with a view to their potential future uses for BTE applications. Nanoceramics vary from typical ceramics due to the reinforcing phase's much higher surface-to-volume ratio and significantly higher characteristic ratio, increased ductility without compromising strength and resistance. During bone regeneration, nanoceramics form an osseointegration surface with the bone, providing a way to investigate such implants *in vivo* conditions. CS provides an ideal environment for cell loading as an ECM-mimicking biopolymer. These tissue engineering structures based on cell-laden CS/ceramics nanocomposites would be more attractive. They may provide potential solutions in 3D porous scaffolds with synergistically enhanced physicochemical and biological characteristics for enhanced bone regeneration. Despite the substantial advancements made in CS-based materials, stability issues still need to be resolved. The full potential of CS-based materials in diverse biomedical applications and the potential of CS in conjunction with other materials need to be investigated. Overall, the combinatorial approach of using CS's adaptability, biocompatibility, and biodegradability, together with the osteoconductive, osteoinductive, and enhanced mechanical features of nano ceramics, make them a promising biocomposite material in the field of BTE.

Abbreviations

ALP	Alkaline phosphatase
BCP	Biphasic calcium phosphate

BG	Bioglass
BMD	Bone mineral density
BMP	Bone morphogenetic protein
BMSC	Bone marrow mesenchymal stem cell
BTE	Bone tissue engineering
CeO_2	Cerium oxide
CS	Chitosan
Dp	Diopside
ECM	Extracellular matrix
GEL	Gelatin
HAp	Hydroxyapatite
mMSCs	Mouse mesenchymal stem cells
nHAp	Nanohydroxyapatite
OC	Osteocalcin
PCL	Polycaprolactone
PEG	Polyethylene glycol
PGA	Polyglycolic acid
PLA	Polylactic acid
PLGA	Poly(lactic-*co*-glycolic) acid
PLLA	Poly(L-lactic) acid
Runx2	Runt-related transcription factor 2
TCP	Tricalcium phosphate
TiO_2	Titanium di-oxide
WH	Whitlockite

Conflicts of interest

There are no conflicts to declare.

References

1 F. A. Tylavsky, L. A. Spence and L. Harkness, *J. Nutr.*, 2008, **138**, 164S–165S.
2 R. Florencio-Silva, G. R. D. S. Sasso, E. Sasso-Cerri, M. J. Simões and P. S. Cerri, *BioMed Res. Int.*, 2015, 421746, DOI: **10.1155/2015/421746**.
3 F. Loi, L. A. Córdova, J. Pajarinen, T. hua Lin, Z. Yao and S. B. Goodman, *Bone*, 2016, **86**, 119–130.
4 X. Chen, Z. Wang, N. Duan, G. Zhu, E. M. Schwarz and C. Xie, *Connect. Tissue Res.*, 2018, **59**, 99–107.
5 E. H. Schemitsch, *J. Orthop. Traumatol.*, 2017, **31**, S20–S22.
6 E. Roddy, M. R. DeBaun, A. Daoud-Gray, Y. P. Yang and M. J. Gardner, *Eur. J. Orthop. Surgery Traumatol.*, 2017, **28**, 351–362.
7 P. P. Patel, C. Buckley, B. L. Taylor, C. C. Sahyoun, S. D. Patel, A. J. Mont, L. Mai, S. Patel and J. W. Freeman, *J. Biomed. Mater. Res., Part A*, 2019, **107**, 732–741.
8 Bone Graft Substitutes Market Size, Share | Global Report, 2029, **https://www.fortunebusinessinsights.com/bone-graft-substitutes-market-103106**, (accessed 30 May 2023).
9 A. H. Schmidt, *Injury*, 2021, **52**, S18–S22.
10 Z. Zhou, H. Zhao, S. Zhang, J. Zheng and C. Yang, *J. Cranio-Maxillofacial Surgery*, 2019, **47**, 6–14.
11 S. R. Konda, C. P. Littlefield, K. D. Carlock, A. Ganta, P. Leucht and K. A. Egol, *Arch. Orthop. Traumatol. Surg.*, 2022, **142**, 961–968.
12 C. P. Miller and C. P. Chiodo, *Foot Ankle Clin.*, 2016, **21**, 825–837.
13 Y. Fillingham and J. Jacobs, *Bone Joint J.*, 2016, **98-B**, 6–9.
14 H. J. Haugen, S. P. Lyngstadaas, F. Rossi and G. Perale, *J. Clin. Periodontol.*, 2019, **46**, 92–102.
15 H. S. Sohn and J. K. Oh, *Biomater. Res.*, 2019, **23**, 1–7.
16 R. L. Huang, E. Kobayashi, K. Liu and Q. Li, *EBioMedicine*, 2016, **12**, 43–54.
17 C. J. Kowalczewski and J. M. Saul, *Front. Pharmacol.*, 2018, **9**, 513.
18 S. Prasadh and R. C. W. Wong, *Oral Sci. Int.*, 2018, **15**, 48–55.
19 S. Sayed1, O. Faruq2 and G. Uzer2, DOI: **10.31031/OOIJ.2022.02.000548**.
20 L. Guo, Z. Liang, L. Yang, W. Du, T. Yu, H. Tang, C. Li and H. Qiu, *J. Controlled Release*, 2021, **338**, 571–582.
21 C. Igwe Idumah, J. T. Nwabanne and F. A. Tanjung, *Cleaner Mater.*, 2021, **2**, 100022.
22 M.-P. Ginebra, M. Espanol, Y. Maazouz, V. Bergez and D. Pastorino, *EFORT Open Rev*, 2018, **3**, 173–183.
23 M. T. Islam, R. M. Felfel, E. A. Abou Neel, D. M. Grant, I. Ahmed and K. M. Z. Hossain, *J. Tissue Eng.*, 2017, DOI: **10.1177/2041731417719170**.
24 N. Baig, I. Kammakakam, W. Falath and I. Kammakakam, *Mater. Adv.*, 2021, **2**, 1821–1871.
25 F. Baino, G. Novajra and C. Vitale-Brovarone, *Front. Bioeng. Biotechnol.*, 2015, **3**, 202.
26 R. de, S. Victor, A. M. da, C. Santos, B. V. de Sousa, G. de, A. Neves, L. N. de, L. Santana and R. R. Menezes, *Materials*, 2020, **13**, 4995.
27 T. Sukpaita, S. Chirachanchai, A. Pimkhaokham and R. S. Ampornaramveth, *Mar. Drugs*, 2021, **19**, 551.
28 F. Barrère, M. Ni, P. Habibovic, P. Ducheyne and K. de Groot, *Tissue Eng.*, 2008, 223–254.
29 P. Dey, *Contemp. Top. Phosphorus Biol. Mater.*, 2020, DOI: **10.5772/INTECHOPEN.92065**.
30 S. Pina, R. Rebelo, V. M. Correlo, J. M. Oliveira and R. L. Reis, *Adv. Exp. Med. Biol.*, 2018, **1058**, 53–75.
31 T. Kim, C. W. See, X. Li and D. Zhu, *Eng. Regener.*, 2020, **1**, 6–18.
32 M. M. Islam, M. Shahruzzaman, S. Biswas, M. Nurus Sakib and T. U. Rashid, *Bioact. Mater.*, 2020, **5**, 164–183.
33 J. S. Fernandes, P. Gentile, R. A. Pires, R. L. Reis and P. V. Hatton, *Acta Biomater.*, 2017, **59**, 2–11.
34 P. Kumar, B. S. Dehiya and A. Sindhu, *Int. J. Appl. Eng. Res.*, 2018, **13**, 2744–2752.
35 I. Khan, K. Saeed and I. Khan, *Arabian J. Chem.*, 2019, **12**, 908–931.
36 T. J. Webster, C. Ergun, R. H. Doremus, R. W. Siegel and R. Bizios, *Biomaterials*, 2000, **21**, 1803–1810.
37 G. Paramasivam, V. V. Palem, T. Sundaram, V. Sundaram, S. C. Kishore and S. Bellucci, *Nanomaterials*, 2021, **11**, 3228.

38 K. Maji and S. Dasgupta, *J. Mater. Res.*, 2019, **34**, 2807–2818.
39 J. Jeong, J. H. Kim, J. H. Shim, N. S. Hwang and C. Y. Heo, *Biomater. Res.*, 2019, **23**, 1–11.
40 G. Fostad, B. Hafell, A. Førde, R. Dittmann, R. Sabetrasekh, J. Will, J. E. Ellingsen, S. P. Lyngstadaas and H. J. Haugen, *J. Eur. Ceram. Soc.*, 2009, **29**, 2773–2781.
41 S. Mandizadeh, F. Soofivand, S. Bagheri and M. Salavati-Niasari, *PLoS One*, 2017, **12**, e0162891.
42 C. Aydin, *J. Mater. Sci.: Mater. Electron.*, 2018, **29**, 20087–20096.
43 R. Liu, M. Liu and J. Chang, *J. Nanopart. Res.*, 2017, **19**, 1–13.
44 J. K. Guo, J. Li and H. M. Kou, *Mod. Inorg. Synth. Chem. (2nd Ed.)*, 2017, 463–492.
45 D. Zhang, C. Du, J. Chen, Q. Shi, Q. Wang, S. Li, W. Wang, X. Yan and Q. Fan, *J. Sol-Gel Sci. Technol.*, 2018, **88**, 422–429.
46 R. Safi, A. Ghasemi, R. Shoja-Razavi, E. Ghasemi and T. Sodaee, *Ceram. Int.*, 2016, **5**, 6375–6382.
47 R. C. F. Cheung, T. B. Ng, J. H. Wong and W. Y. Chan, *Mar. Drugs*, 2015, **13**, 5156–5186.
48 C. Pardo-Castaño and G. Bolaños, *J. Supercrit. Fluids*, 2019, **151**, 63–74.
49 C. Brasselet, G. Pierre, P. Dubessay, M. Dols-Lafargue, J. Coulon, J. Maupeu, A. Vallet-Courbin, H. de Baynast, T. Doco, P. Michaud and C. Delattre, *Appl. Sci.*, 2019, **9**, 1321.
50 S. Kim, *Int. J. Polym. Sci.*, 2018, **1**(13), DOI: **10.1155/2018/1708172**.
51 M. B. Kaczmarek, K. Struszczyk-Swita, X. Li, M. Szczęsna-Antczak and M. Daroch, *Front. Bioeng. Biotechnol.*, 2019, **7**, 243.
52 H. El Knidri, R. El Khalfaouy, A. Laajeb, A. Addaou and A. Lahsini, *Process Saf. Environ. Prot.*, 2016, **104**, 395–405.
53 M. Kozma, B. Acharya and R. Bissessur, *Polymers*, 2022, **14**, 3989.
54 J. Bonilla, A. M. Q. B. Bittante and P. J. A. Sobral, *J. Therm. Anal. Calorim.*, 2017, **130**, 1221–1227.
55 Y. Cao, Y. F. Tan, Y. S. Wong, M. W. J. Liew and S. Venkatraman, *Mar. Drugs*, 2019, **17**, 381.
56 A. Di Martino, M. Sittinger and M. V. Risbud, *Biomaterials*, 2005, **26**, 5983–5990.
57 S. K. L. Levengood and M. Zhang, *J. Mater. Chem. B*, 2014, **2**, 3161.
58 H. M. Ibrahim, E. M. R. E. Zairy, H. M. Ibrahim and E. M. R. E. Zairy, *Concepts, Compd. Altern. Antibact.*, 2015, DOI: **10.5772/61300**.
59 M. L. Tan, P. Shao, A. M. Friedhuber, M. van Moorst, M. Elahy, S. Indumathy, D. E. Dunstan, Y. Wei and C. R. Dass, *Biomaterials*, 2014, **35**, 7828–7838.
60 F. Liu, H. Y. Li, Z. Wang, H. N. Zhang, Y. Z. Wang and H. Xu, *BMC Musculoskeletal Disord.*, 2020, **21**, 1–10.
61 D. Diekjürgen and D. W. Grainger, *Biomaterials*, 2017, **141**, 96–115.
62 V. R. Hokmabad, S. Davaran, M. Aghazadeh, E. Alizadeh, R. Salehi and A. Ramazani, *Tissue Eng. Regener. Med.*, 2018, **15**, 735–750.
63 B. Li, J. Elango and W. Wu, *Appl. Sci.*, 2020, **10**, 4719.
64 C. Y. Hsieh, S. P. Tsai, D. M. Wang, Y. N. Chang and H. J. Hsieh, *Biomaterials*, 2005, **26**, 5617–5623.
65 H. Y. Jung, P. Le Thi, K. H. HwangBo, J. W. Bae and K. D. Park, *Carbohydr. Polym.*, 2021, **261**, 117810.
66 S. Deepthi, J. Venkatesan, S. K. Kim, J. D. Bumgardner and R. Jayakumar, *Int. J. Biol. Macromol.*, 2016, **93**, 1338–1353.
67 (7) (PDF) Bioinert Ceramics for Biomedical Applications, **https://www.researchgate.net/publication/338253271_Bioinert_Ceramics_for_Biomedical_Applications**, (accessed 30 May 2023).
68 V. Sansone, D. Pagani and M. Melato, *Clin. Cases Mineral Bone Metabolism*, 2013, **10**, 34.
69 V. Babuska, P. B. Kasi, P. Chocholata, L. Wiesnerova, J. Dvorakova, R. Vrzakova, A. Nekleionova, L. Landsmann and V. Kulda, *Appl. Sci.*, 2022, **12**, 6793.
70 G. G. Walmsley, A. McArdle, R. Tevlin, A. Momeni, D. Atashroo, M. S. Hu, A. H. Feroze, V. W. Wong, P. H. Lorenz, M. T. Longaker and D. C. Wan, *Nanomedicine*, 2015, **11**, 1253–1263.
71 X. Yu, X. Tang, S. V. Gohil and C. T. Laurencin, *Adv. Healthcare Mater.*, 2015, **4**, 1268–1285.
72 R. Ikono, N. Li, N. H. Pratama, A. Vibriani, D. R. Yuniarni, M. Luthfansyah, B. M. Bachtiar, E. W. Bachtiar, K. Mulia, M. Nasikin, H. Kagami, X. Li, E. Mardliyati, N. T. Rochman, T. Nagamura-Inoue and A. Tojo, *Biotechnol. Rep.*, 2019, **24**, e00350.
73 P. Kumar, *Int. J. Biomater.*, 2018, 1–7, DOI: **10.1155/2018/6576157**.
74 C. H. Valencia-Llano, M. A. Solano and C. D. Grande-Tovar, *Polymers*, 2021, **13**(22), 3877, DOI: **10.3390/POLYM13223877**.
75 K. Balagangadharan, S. Viji Chandran, B. Arumugam, S. Saravanan, G. Devanand Venkatasubbu and N. Selvamurugan, *Int. J. Biol. Macromol.*, 2018, **111**, 953–958.
76 S. Pattnaik, S. Nethala, A. Tripathi, S. Saravanan, A. Moorthi and N. Selvamurugan, *Int. J. Biol. Macromol.*, 2011, **49**, 1167–1172.
77 A. Bhowmick, N. Pramanik, P. Jana, T. Mitra, A. Gnanamani, M. Das and P. P. Kundu, *Int. J. Biol. Macromol.*, 2017, **95**, 348–356.
78 E. B. Toloue, S. Karbasi, H. Salehi and M. Rafienia, *Mater. Sci. Eng., C*, 2019, **99**, 1075–1091.
79 A. Teimouri, R. Ebrahimi, A. N. Chermahini and R. Emadi, *RSC Adv.*, 2015, **5**, 27558–27570.
80 V. S. de Viteri, E. Fuentes, V. S. de Viteri and E. Fuentes, *Tribol.: Fundam. Adv.*, 2013, DOI: **10.5772/55860**.
81 J. Ferin, G. Oberdörster and D. P. Penney, *Am. J. Respir. Cell Mol. Biol.*, 1992, **6**, 535–542.
82 Y. Ren, X. Feng, X. Lang, J. Wang, Z. Du and X. Niu, *J. Nanomater.*, 2020, **2020**, DOI: **10.1155/2020/8887323**.
83 C. H. Valencia-Llano, M. A. Solano and C. D. Grande-Tovar, *Polymers*, 2021, **13**, 3877.
84 A. Hashemi, M. Ezati, J. Mohammadnejad, B. Houshmand and S. Faghihi, *Int. J. Nanomed.*, 2020, **15**, 4471–4481.
85 B. Kolathupalayam Shanmugam, S. Rangaraj, K. Subramani, S. Srinivasan, W. K. Aicher and R. Venkatachalam, *Mater. Sci. Eng., C*, 2020, **110**, DOI: **10.1016/J.MSEC.2020.110710**.

86 X. Yin, C. Yang, Z. Wang, Y. Zhang, Y. Li, J. Weng and B. Feng, *Mater. Sci. Eng., C*, 2021, **124**, 112087.
87 A. R. Walpole, Z. Xia, C. W. Wilson, J. T. Triffitt and P. R. Wilshaw, *J. Biomed. Mater. Res., Part A*, 2009, **90A**, 46–54.
88 S. Ni, C. Li, S. Ni, T. Chen and T. J. Webster, *Int. J. Nanomed.*, 2014, **9**, 3325–3334.
89 C. Hadjicharalambous, O. Prymak, K. Loza, A. Buyakov, S. Kulkov and M. Chatzinikolaidou, *Front. Bioeng. Biotechnol.*, 2015, **3**, 175.
90 A. Teimouri, R. Ebrahimi, A. N. Chermahini and R. Emadi, *RSC Adv.*, 2015, **5**, 27558–27570.
91 E. B. Toloue, S. Karbasi, H. Salehi and M. Rafienia, *Mater. Sci. Eng., C*, 2019, **99**, 1075–1091.
92 R. Depprich, H. Zipprich, M. Ommerborn, C. Naujoks, H. P. Wiesmann, S. Kiattavorncharoen, H. C. Lauer, U. Meyer, N. R. Kübler and J. Handschel, *Head Face Med.*, 2008, **4**(30), DOI: 10.1186/1746-160X-4-30.
93 A. Mftah, F. H. Alhassan, M. S. Al-Qubaisi, M. E. El Zowalaty, T. J. Webster, M. Sh-Eldin, A. Rasedee, Y. H. Taufiq-Yap and S. S. Rashid, *Int. J. Nanomed.*, 2015, **10**, 765–774.
94 R. Jayakumar, R. Ramachandran, P. T. Sudheesh Kumar, V. V. Divyarani, S. Srinivasan, K. P. Chennazhi, H. Tamura and S. V. Nair, *Int. J. Biol. Macromol.*, 2011, **49**, 274–280.
95 K. Balagangadharan, S. Viji Chandran, B. Arumugam, S. Saravanan, G. Devanand Venkatasubbu and N. Selvamurugan, *Int. J. Biol. Macromol.*, 2018, **111**, 953–958.
96 E. E. A. Mohammed, H. H. Beherei, M. El-Zawahry, A. R. H. Farrag, N. Kholoussi, I. Helwa, K. Gaber, M. A. Allam, M. Mabrouk and A. K. A. Aleem, *Open Access Maced J. Med. Sci.*, 2019, **7**, 2739.
97 S. Dhivya, S. Saravanan, T. P. Sastry and N. Selvamurugan, *J. Nanobiotechnol.*, 2015, **13**, 1–13.
98 J. Ji, X. Tong, X. Huang, T. Wang, Z. Lin, Y. Cao, J. Zhang, L. Dong, H. Qin and Q. Hu, *Biomed. Mater.*, 2015, **10**, 045005.
99 J. S. Lee, S. D. Baek, J. Venkatesan, I. Bhatnagar, H. K. Chang, H. T. Kim and S. K. Kim, *Int. J. Biol. Macromol.*, 2014, **67**, 360–366.
100 P. Ye, B. Yu, J. Deng, R. F. She and W. L. Huang, *Exp. Ther. Med.*, 2017, **14**, 5547–5553.
101 H. Wu, P. Lei, G. Liu, Y. S. Zhang, J. Yang, L. Zhang, J. Xie, W. Niu, H. Liu, J. Ruan, Y. Hu and C. Zhang, *Sci. Rep.*, 2017, **7**, 1–14.
102 H. Jiang, Y. Zuo, Q. Zou, H. Wang, J. Du, Y. Li and X. Yang, *ACS Appl. Mater. Interfaces*, 2013, **5**, 12036–12044.
103 S. qiang Ruan, J. Deng, L. Yan and W. liang Huang, *Biomed. Pharmacother.*, 2018, **97**, 600–606.
104 Y. Zhou, X. Liu, H. She, R. Wang, F. Bai and B. Xiang, *Regener. Ther.*, 2022, **21**, 307–321.
105 L. Yang, J. Huang, S. Yang, W. Cui, J. Wang, Y. Zhang, J. Li and X. Guo, *ACS Biomater. Sci. Eng.*, 2018, **4**, 3246–3258.
106 L. L. Hench, *J. Mater. Sci.: Mater. Med.*, 2006, **17**, 967–978.
107 S. A. Ferreira, G. Young, J. R. Jones and S. Rankin, *Mater. Sci. Eng., C*, 2021, **118**, 111393.
108 S. Behzadi, Y. Mohammadi, L. Rezaei-Soufi and A. Farmany, *Clin. Oral. Investig.*, 2022, **26**, 6061–6078.
109 A. B. Workie and S. J. Shih, *RSC Adv.*, 2022, **12**, 23143–23152.
110 M. Maximov, O. C. Maximov, L. Craciun, D. Ficai, A. Ficai and E. Andronescu, *Coatings*, 2021, **11**, 1386.
111 U. Pantulap, M. Arango-Ospina and A. R. Boccaccini, *J. Mater. Sci.: Materi. Med.*, 2021, **33**, 1–41.
112 J. Yang, T. Long, N. F. He, Y. P. Guo, Z. A. Zhu and Q. F. Ke, *J. Mater. Chem. B*, 2014, **2**, 6611–6618.
113 R. Ravarian, M. Craft and F. Dehghani, *J. Biomed. Mater. Res., Part A*, 2015, **103**, 2898–2908.
114 S. Singh, G. Singh, N. Bala and K. Aggarwal, *Int. J. Biol. Macromol.*, 2020, **151**, 519–528.
115 T. Jiang, Z. Zhang, Y. Zhou, Y. Liu, Z. Wang, H. Tong, X. Shen and Y. Wang, *Biomacromolecules*, 2010, **11**, 1254–1260.
116 M. Parvizifard and S. Karbasi, *Int. J. Biol. Macromol.*, 2020, **152**, 645–662.
117 W. Li, Y. Ding, S. Yu, Q. Yao and A. R. Boccaccini, *ACS Appl. Mater. Interfaces*, 2015, **7**, 20845–20854.
118 S. K. Mohonta, K. H. Maria, S. Rahman, H. Das and S. M. Hoque, *Int. Nano Lett.*, 2021, **11**, 381–393.
119 E. Pepla, L. K. Besharat, G. Palaia, G. Tenore and G. Migliau, *Ann. Stomatol.*, 2014, **5**, 108.
120 B. H. Atak, B. Buyuk, M. Huysal, S. Isik, M. Senel, W. Metzger and G. Cetin, *Carbohydr. Polym.*, 2017, **164**, 200–213.
121 Z. Zhang, G. Wu, Y. Cao, C. Liu, Y. Jin, Y. Wang, L. Yang, J. Guo and L. Zhu, *Mater. Sci. Eng., C*, 2018, **93**, 445–454.
122 S. Batool, U. Liaqat, B. Babar and Z. Hussain, *J. Korean Ceram. Soc.*, 2021, **58**, 530–547.
123 H. Cheng, R. Chabok, X. Guan, A. Chawla, Y. Li, A. Khademhosseini and H. L. Jang, *Acta Biomater.*, 2018, **69**, 342–351.
124 F. Xiao, J. Shi, X. Zhang, M. Hu, K. Chen, C. Shen, X. Chen, Y. Guo and Y. Li, *Front. Bioeng. Biotechnol.*, 2023, **11**, 1071692.
125 H. Li, P. Xia, S. Pan, Z. Qi, C. Fu, Z. Yu, W. Kong, Y. Chang, K. Wang, D. Wu and X. Yang, *Int. J. Nanomed.*, 2020, **15**, 7199–7214.
126 A. F. Bonciu, S. Orobeti, L. E. Sima, M. Icriverzi, M. Filipescu, A. Moldovan, A. Popescu, V. Dinca and M. Dinescu, *Appl. Surf. Sci.*, 2020, **533**, 147464.
127 J. Shan, S. Wang, H. Xu, H. Zhan, Z. Geng, H. Liang and M. Dai, *J. Biomater. Appl.*, 2022, **36**, 976–984.
128 S. Bhushan, S. Singh, T. K. Maiti, A. Das, A. Barui, L. R. Chaudhari, M. G. Joshi and D. Dutt, *Int. J. Biol. Macromol.*, 2023, **236**, DOI: 10.1016/J.IJBIOMAC.2023.123813.
129 D. De Meo, L. Yildizbakan, N. Iqbal, P. Ganguly, E. Kumi-Barimah, T. Do, E. Jones, P. V. Giannoudis and A. Jha, *Antibiotics*, 2023, **12**, 1004.
130 C. Wu, Y. Ramaswamy and H. Zreiqat, *Acta Biomater.*, 2010, **6**, 2237–2245.
131 S. Pang, D. Wu, F. Kamutzki, J. Kurreck, A. Gurlo and D. A. H. Hanaor, *Mater. Des.*, 2022, **215**, 110480.
132 J. P. Kumar, L. Lakshmi, V. Jyothsna, D. R. P. Balaji, S. Saravanan, A. Moorthi and N. Selvamurugan, *J. Biomed. Nanotechnol.*, 2014, **10**, 970–981.

133 Y. P. Singh, S. Dasgupta and R. Bhaskar, *J. Biomater. Sci., Polym. Ed.*, 2019, **30**, 1756–1778.
134 K. H. Park, S. J. Kim, Y. H. Jeong, H. J. Moon, H. J. Song and Y. J. Park, *Mater. Sci. Eng., C*, 2018, **90**, 113–118.
135 M. Matinfar, A. S. Mesgar and Z. Mohammadi, *Mater. Sci. Eng., C*, 2019, **100**, 341–353.
136 K. Maji, S. Dasgupta, K. Pramanik and A. Bissoyi, *Mater. Sci. Eng., C*, 2018, **86**, 83–94.
137 N. Siddiqui, K. Pramanik and E. Jabbari, *Mater. Sci. Eng., C*, 2015, **54**, 76–83.
138 N. Siddiqui, S. Madala, S. Rao Parcha and S. P. Mallick, *Biomed. Phys. Eng. Express*, 2020, **6**, 015018.
139 N. Siddiqui, S. Madala, S. Rao Parcha and S. P. Mallick, *Biomed. Phys. Eng. Express*, 2020, **6**, 015018.
140 K. Maji, S. Dasgupta, K. Pramanik and A. Bissoyi, *Mater. Sci. Eng., C*, 2018, **86**, 83–94.
141 I. R. Serra, R. Fradique, M. C. S. Vallejo, T. R. Correia, S. P. Miguel and I. J. Correia, *Mater. Sci. Eng., C*, 2015, **55**, 592–604.
142 Y. Yin, F. Ye, J. Cui, F. Zhang, X. Li and K. Yao, *J. Biomed. Mater. Res., Part A*, 2003, **67**, 844–855.
143 S. Keikhaei, Z. Mohammadalizadeh, S. Karbasi and A. Salimi, *Mater Technol*, 2019, **34**, 615–625, DOI: **10.1080/10667857.2019.1611053**.
144 D. S. Amarasekara, S. Kim and J. Rho, *Int. J. Mol. Sci.*, 2021, **22**, 1–16.
145 B. Farhadihosseinabadi, A. Zarebkohan, M. Eftekhary, M. Heiat, M. Moosazadeh Moghaddam and M. Gholipourmalekabadi, *Cell. Mol. Life Sci.*, 2019, **76**, 2697–2718.
146 H. Hu, P. Zhao, J. Liu, Q. Ke, C. Zhang, Y. Guo and H. Ding, *J. Nanobiotechnol.*, 2018, **16**, 1–13.
147 W. Sun, M. Li, Y. Zhang, Y. Huang, Q. Zhan, Y. Ren, H. Dong, J. Chen, Z. Li, C. Fan, F. Huang, Z. Shen and Z. Jiang, *Biomed. Pharmacother.*, 2021, **138**, 111480.
148 Y. Wagley, A. Chesi, P. K. Acevedo, S. Lu, A. D. Wells, M. E. Johnson, S. F. A. Grant and K. D. Hankenson, *Stem Cells*, 2020, **38**, 1332–1347.
149 J. W. Lowery and V. Rosen, *Physiol. Rev.*, 2018, **98**, 2431–2452.
150 M. S. Rahman, N. Akhtar, H. M. Jamil, R. S. Banik and S. M. Asaduzzaman, *Bone Res.*, 2015, **3**, 1–20.
151 T. Katagiri and T. Watabe, *Cold Spring Harb Perspect. Biol.*, 2016, **8**, a021899.
152 B. Khorsand, S. Elangovan, L. Hong, A. Dewerth, M. S. D. Kormann and A. K. Salem, *AAPS J.*, 2017, **19**, 438–446.
153 J. Wang, M. Wang, F. Chen, Y. Wei, X. Chen, Y. Zhou, X. Yang, X. Zhu, C. Tu and X. Zhang, *Int. J. Nanomed.*, 2019, **14**, 7987.
154 H. Liu, H. Peng, Y. Wu, C. Zhang, Y. Cai, G. Xu, Q. Li, X. Chen, J. Ji, Y. Zhang and H. W. OuYang, *Biomaterials*, 2013, **34**, 4404–4417.
155 J. T. Zieba, Y. T. Chen, B. H. Lee and Y. Bae, *Biomolecules*, 2020, **10**, 332.
156 M. P. Yavropoulou and J. G. Yovos, *Hormones*, 2014, **13**, 24–37.
157 J. Tao, S. Chen and B. Lee, *Ann. N. Y. Acad. Sci.*, 2010, **1192**, 257–268.
158 J. Regan and F. Long, *Curr. Osteop. Rep.*, 2013, **11**, 126–129.
159 Z. Zou, L. Wang, Z. Zhou, Q. Sun, D. Liu, Y. Chen, H. Hu, Y. Cai, S. Lin, Z. Yu, B. Tan, W. Guo, Z. Ling and X. Zou, *Bioact. Mater.*, 2021, **6**, 1839–1851.
160 Y. Wang, J. Pan, Y. Zhang, X. Li, Z. Zhang, P. Wang, Z. Qin and J. Li, *J. Biomed. Mater. Res., Part B: Appl. Biomater.*, 2019, **107**, 149–160.
161 N. Chakravorty, S. Hamlet, A. Jaiprakash, R. Crawford, A. Oloyede, M. Alfarsi, Y. Xiao and S. Ivanovski, *Clin. Oral. Implants Res.*, 2014, **25**, 475–486.
162 W. Gong, Y. Dong, S. Wang, X. Gao and X. Chen, *RSC Adv.*, 2017, **7**, 13760–13767.
163 H. Zhang, L. F. Cooper, X. Zhang, Y. Zhang, F. Deng, J. Song and S. Yang, *RSC Adv.*, 2016, **6**, 44062–44069.
164 U. Saran, S. Gemini Piperni and S. Chatterjee, *Arch. Biochem. Biophys.*, 2014, **561**, 109–117.
165 M. Arango-Ospina, Q. Nawaza and A. R. Boccaccini, *Nanostruct. Biomater. Regener. Med.*, 2020, 255–273.
166 D. Zhu, B. Lu, Q. Yang, H. Yu, P. Liu, J. Yin, Y. Chen, Y. Huang, Q. Ke, C. Zhang, Y. Guo and Y. Gao, *Chem. Eng. J.*, 2021, **405**, 127077.